(12) LEVEL II

USAAVRADCOM-TR-80-D-2

AD A082443

THE DESIGN, FABRICATION, AND TEST OF AN ELECTROFLUIDIC SERVOVALVE

Maurice F. Funke, Lester K. Pecan
TriTec, Inc.
P. O. Box 56
Columbia, Maryland 21045

February 1980

Final Report for Period September 1978 - October 1979

Prepared for
APPLIED TECHNOLOGY LABORATORY
U.S. ARMY RESEARCH AND TECHNOLOGY LABORATORIES (AVRADCOM)
Fort Eustis, Va. 23604

APPLIED TECHNOLOGY LABORATORY POSITION STATEMENT

This report has been reviewed by the Applied Technology Laboratory, US Army Research and Technology Laboratories (AVRADCOM), and is considered to be technically sound.

This research effort resulted from the need which exists to develop a dual input (electrical and fluidic) servovalve for military vehicles. The potential exists for eventually equipping these vehicles with electrical or fluidic controlling systems as well as combination systems. An electro-fluidic servovalve would provide the US Army with the capability of transforming electrical or fluidic control input signals into mechanical motion of a single servoactuator rather than two separate servoactuators, thereby reducing cost, weight, and complexity.

Mr. George W. Fosdick of the Applied Aeronautics Technical Area, Aeronautical Systems Division, served as project engineer for this effort.

UNCLASSIFIED

SECURITY CLASSIFICATION OF THIS PAGE (When Data Entered)

REPORT DOCUMENTATION PAGE

READ INSTRUCTIONS BEFORE COMPLETING FORM

1. REPORT NUMBER: USAAVRADCOM-TR-80-D-2
2. GOVT ACCESSION NO.
3. RECIPIENT'S CATALOG NUMBER

4. TITLE (and Subtitle): THE DESIGN, FABRICATION, AND TEST OF AN ELECTROFLUIDIC SERVOVALVE
5. TYPE OF REPORT & PERIOD COVERED: Final Report, Sep 1978 — Oct 1979
6. PERFORMING ORG. REPORT NUMBER

7. AUTHOR(s): Maurice F. Funke, Lester K. Pecan
8. CONTRACT OR GRANT NUMBER(s): DAAK51-78-C-0022

9. PERFORMING ORGANIZATION NAME AND ADDRESS: TriTec, Inc., P. O. Box 56, Columbia, Maryland 21045
10. PROGRAM ELEMENT, PROJECT, TASK AREA & WORK UNIT NUMBERS: 62120A 1L162120AH25 00 003 EK

11. CONTROLLING OFFICE NAME AND ADDRESS: Applied Technology Laboratory, U. S. Army Research and Technology Laboratories (AVRADCOM), Fort Eustis, Virginia 23604
12. REPORT DATE: February 1980
13. NUMBER OF PAGES: 55

14. MONITORING AGENCY NAME & ADDRESS(if different from Controlling Office)
15. SECURITY CLASS. (of this report): UNCLASSIFIED
15a. DECLASSIFICATION/DOWNGRADING SCHEDULE

16. DISTRIBUTION STATEMENT (of this Report)

Approved for public release; distribution unlimited.

17. DISTRIBUTION STATEMENT (of the abstract entered in Block 20, if different from Report)

18. SUPPLEMENTARY NOTES

19. KEY WORDS (Continue on reverse side if necessary and identify by block number)

Electrofluidic Servovalves	Hydrofluidics
Fluerics	Servoactuators
Fluidics	Servovalves
Flight Control Systems	Stability Augmentation Systems

20. ABSTRACT (Continue on reverse side if necessary and identify by block number)

This report covers the design, fabrication, and testing of a dual input (hydraulic and electric) servovalve using fluidic amplifiers and positive derivative feedback. The design utilized a two-stage gain block to drive a hydraulic actuator. Electrical input signals were converted by a torque motor into mechanical motion of the first-stage flow splitter. Actuator position was fed back to a movable splitter in the second-stage amplifier. Flow to the actuator was augmented in a positive feedback sense by a spool

DD FORM 1 JAN 73 1473 EDITION OF 1 NOV 65 IS OBSOLETE

UNCLASSIFIED

SECURITY CLASSIFICATION OF THIS PAGE (When Data Entered)

395 715

20. Abstract (Cont.)

valve whose flow was proportional to actuator velocity. Performance tests showed that the servovalve accepted and summed combinations of pressure and electrical inputs. Frequency response objectives were met without the high leakage flow penalty usually associated with this application of fluid amplifiers.

SUMMARY

The concept of a dual input (hydraulic and electric) servovalve using fluidic amplifiers and positive derivative feedback was defined and compared with existing designs. A mathematical model was developed and performance predictions were made. Based on the mathematical model, a breadboard servovalve was designed and built. The design utilized a two-stage fluidic gain block driving a hydraulic actuator. Electrical control signals were converted by a torque motor into translation of a movable flow splitter in the first-stage amplifier. Actuator position was fed back by a mechanical link to a movable splitter in the second-stage amplifier. The need for adequate flow to the actuator was met by use of a spool valve to augment the driving amplifier output flow. The spool valve was driven by a piston coupled to the actuator. A variable resistor to ground between the piston and spool valve was used to control the spool response so that flow to the actuator was proportional to actuator velocity in the positive feedback sense.

Performance tests on the servovalve demonstrated the feasibility of the concept. The servovalve accepted and summed combinations of electrical and pressure inputs with predictable outputs. Response tests showed that the desired speed of response was obtained without the leakage penalty usually associated with this application of fluidic amplifiers. Further, it was shown that accurate command position was obtained by direct position feedback to the amplifier jet.

PREFACE

This document is the final report on a program to design, fabricate, and test an electrofluidic servovalve. The work was performed by TriTec, Inc., during the period of September 1978 through October 1979, under Contract DAAK51-78-C-0022. The Applied Technology Laboratory, U.S. Army Research and Technology Laboratories, Fort Eustis, Virgini , sponsored the program, with Mr. George Fosdick as the Contracting Officer's Technical Representative. Acknowledgment is given to Mr. Vincent F. Neradka of TriTec, Inc. and Mr. Francis M. Manion of Rockville, Maryland, who developed the theory underlying the positive derivative feedback concept and provided technical consultation for the program.

TABLE OF CONTENTS

LIST OF ILLUSTRATIONS

INTRODUCTION

Recent interest in hydrofluidic servovalves has been keen as evidenced by the flight qualification of such a system for Army helicopter use. Specifically, the servovalve described herein is intended as a backup system which does not rely on electrical power as do the primary flight control systems. Unfortunately, efforts to date have resulted in servovalves which suffer from high leakage flow, low speed of response, and feedback sensitivity to pressure and/or temperature. This report describes the design and analysis of a servovalve which can accept fluidic, mechanical, and electrical input signals. This valve, while consuming less leakage flow than other fluidic designs, uniquely offers speed-of-response heretofore unattainable. Also, in contrast to other fluidic designs, its position feedback mechanism is insensitive to pressure and temperature variations. Lastly, the servovalve damping can be adjusted to tailor the valve to a particular system in order to optimize system performance.

PHYSICAL DESCRIPTION

The basic configuration of the servovalve is shown in Figure 1. As can be seen from the upper portion of the figure, input to the valve may be mechanical through the jet-pipe, and/or fluidic through the fluidic amplifiers, or electrical through the torquemotor. These inputs, singly or collectively, serve to deflect the final power jet.

Deflection of this jet relative to the splitter produces a differential pressure across the actuator. This pressure is expressed as the sum

$$dP = (\partial P/\partial x_j)dx_j + (\partial P/\partial i)di + (\partial P/\partial P_c)dP_c + (\partial P/\partial x_a)dx_a \qquad (1)$$

mechanical input, jet pipe	electrical input, torque motor	pressure input, fluidic command	load position feedback
← inputs →			

where x_j is jet pipe motion and $\partial P/\partial x_j$ is jet pipe characteristic

i is electrical current input and $\partial P/\partial i$ is the torquemotor characteristic with the fluid amplifier

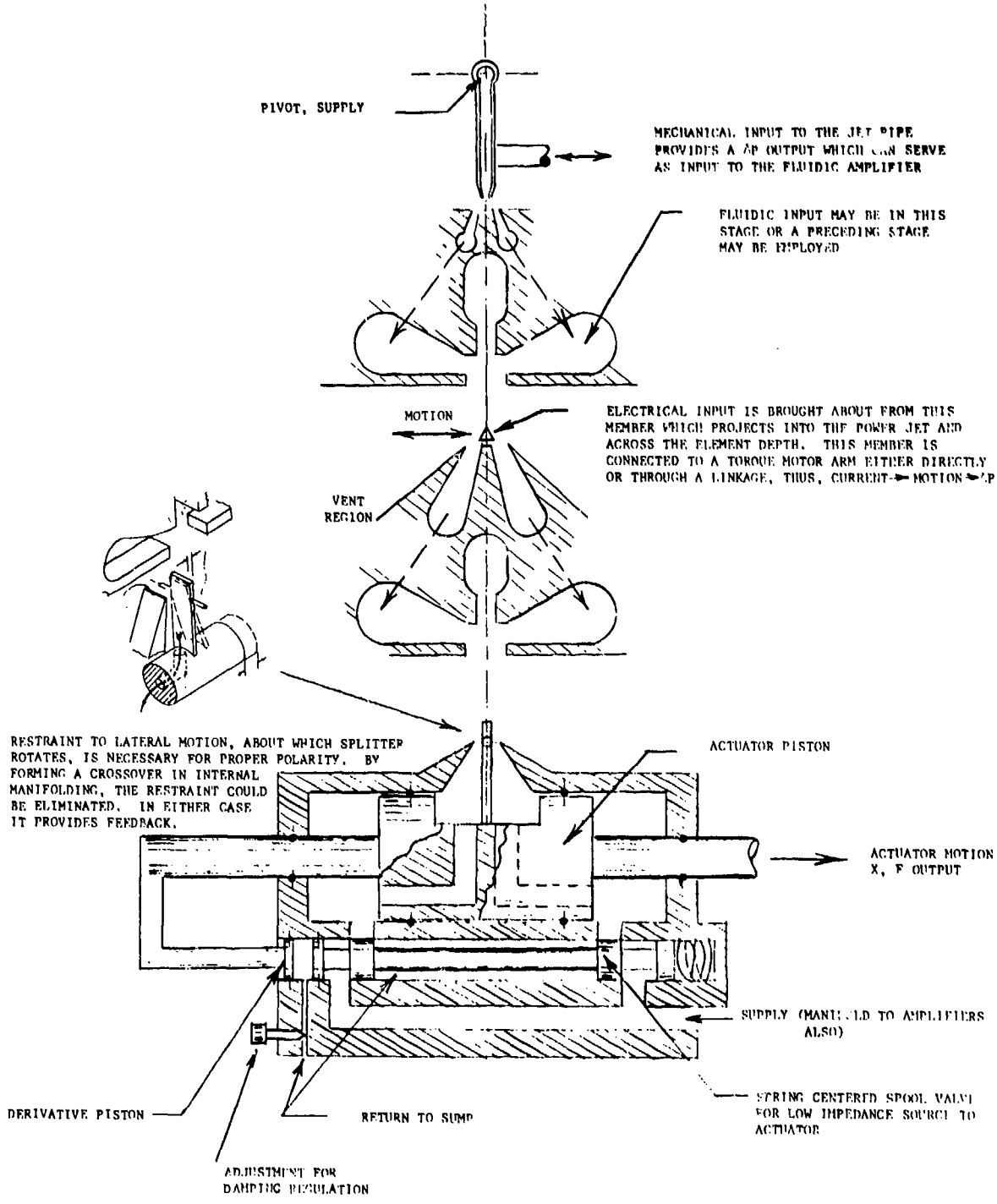

FIGURE 1. SCHEMATIC OF SERVOACTUATOR

P_c is fluidic pressure input and $\partial P/\partial P_c$ is the amplifier gain

x_a is the load position and $\partial P/\partial x_a$ is the pressure differential due to splitter movement

A crucial element to the functioning of this servovalve is that a differential load pressure can be modulated by the motion of a splitter (i.e., $\partial P/\partial x_a$).

A command from any of the inputs (dx_j, di, or dP_c) causes a differential output pressure to develop across the actuator piston faces. This pressure, acting on actuator piston area A_A gives rise to a force unbalance across the actuator piston. The force initiates actuator piston motion. If a small fluidic element is used as a driver amplifier in order to reduce leakage flow within the amplifier, the driving response is low. To overcome this speed of response problem, large driving fluidic elements have previously been used, and a large leakage flow penalty was incurred.

Both an improved speed of response and lower leakage flow can be simultaneously achieved. Referring once again to Figure 1, note that actuator piston motion displaces fluid from the derivative piston cavity. With the adjustment for damping regulation closed, the actuator piston causes 1:1 motion of the spring-centered spool in the low impedance flow valve. This motion opens spool porting to the actuator piston, admitting fluid flow in a positive feedback sense. Adjustment of the damping regulation controls the magnitude of this positive feedback. The positive feedback becomes derivative in nature (a function of $\dot{x}_a$, not x_a), thus reducing the system damping*. With the initiating driver amplifier flow augmented by the low impedance spool flow, a highly responsive actuator piston motion is achieved.

The actuator piston motion will stop at the command position due to the load-position-feedback signal as shown in the right-hand side of Equation (1). Prior hydrofluidic servovalves used various flapper nozzle configurations to provide a load-displacement feedback signal. All of these suffer from temperature and pressure variations, thus degrading system accuracy. In the servovalve

---

* Note that a high impedance driver amplifier results in a severely overdamped system so that some positive feedback is effective in reducing the system damping.

concept presented herein, mechanical position feedback driven by the actuator piston itself is directly used to alter the pressure signal to the actuator piston. This is achieved with a flow splitter, one end of which is attached to the actuator piston (See Figure 1). The other end of the flow-splitter is free to move relative to the amplifier power jet. As the actuator piston moves, the splitter moves in the amplifier power jet, thereby reducing the dP signal which arose from the inputs (dx_j, di, dP_c). Once the dP signal is zero, the actuator piston is motionless and the low impedance spool valve is closed by the centering spring. It must be realized that the spool valve port area, and hence the flow, is dependent not on the dP signal across the actuator piston, but on the rate of actuator piston travel only. In order for the system to have stability and high speed of response, while being driven from small (high impedance) fluidic elements, its components must be properly sized. This is the subject of the following section.

DEVELOPMENT OF THE MATHEMATICAL MODEL

Neglecting nonlinearities due to spool valve overlap, spool leakage, etc., the block diagram which represents the concept shown in Figure 1 is presented in Figure 2.

The input (dx_j, di, dP_c) to the valve gives rise to a jet deflection (y). Through the amplifier characteristic dP_o/dy, a pressure differential exists across the splitter. This pressure across the input resistance of the actuator cylinder generates a flow into the actuator cylinder. By virtue of the volume, flow is integrated, thereby developing a differential pressure across the actuator piston. This differential pressure feeds back to the input summing junction to reduce the dP across the driving amplifier output resistor. This differential pressure acts on the actuator piston area A_A to develop a net force differential across the actuator piston. This force, divided by the load impedance Z_ℓ, defines the actuator piston displacement x_a. This actuator piston displacement feeds back on the actuator flow summing junction in two ways: the swept volume and the derivative feedback.

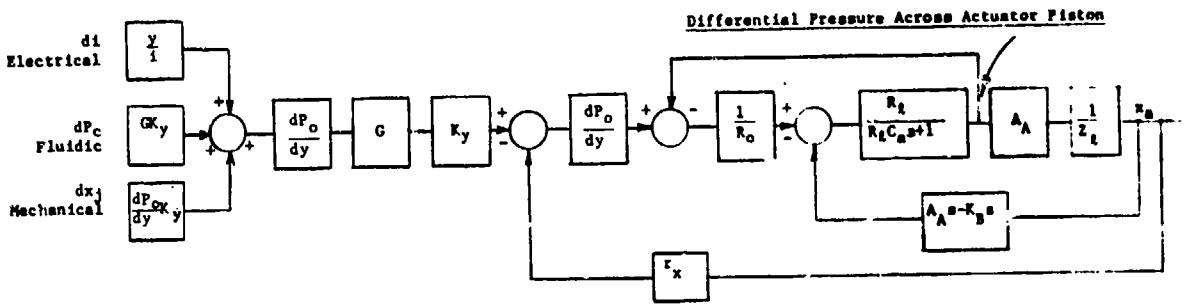

FIGURE 2. SERVOVALVE BLOCK DIAGRAM

where

$\frac{y}{i}$ = Torque motor displacement coefficient, in./amp

G = Pressure gain

K_y = Jet displacement at splitter for pressure input, in./psi

$\frac{dP_o}{dy}$ = Output difference pressure (blocked output) for jet displacement at splitter, psi/in.

R_o = Driving amplifier output resistance, lb sec/in.^{5}

R_ℓ = Leakage resistance across actuator, lb sec/in.^{5}

C_a = Actuator compliance, in.^{3}/psi

A_A = Actuator piston area, in.^{2}

Z_ℓ = Load impedance, lb/in.

r_x = Position feedback ratio

K_B = Derivative feedback, in.^{2}

s = Laplace operator, sec.$^{-1}$

The feedback block $A_As - K_Bs$ is a significant feature. The A_As term is the swept volume flow and represents a system damping element common to all servovalves. For small fluidic element inputs it results in severe overdamping. The A_As gives rise to a time constant which must simply be accepted as a valve response limiting factor. However, the K_Bs of the positive derivative control provides a means of offsetting this inherent servovalve limitation. It also provides a means of eliminating the lag of the swept

volume of actuator piston motion. Thus, not only can damping be tailored to achieve optimum system performance but system speeds-of-response heretofore impossible can be attained, as will be shown in later examples.

Closing the loop between actuator piston position x_a and input jet deflection is the feedback element r_x. Note that this term scales the actuator piston displacement to allow a larger range of gain or x_a to exist. The system designer can adjust the value of r_x by adjusting the location of the position feedback mechanism pivot point to amplify or attenuate the actuator piston displacement.

Note also that the outer loop position feedback is the splitter. It is unaffected by temperature and pressure changes. Previous hydrofluidic servovalves have had feedback gain change with temperature due to viscosity since load motion was transduced into a fluid signal and this signal was processed by viscous elements before it reached the actuator. The use of a splitter coupled to the load avoids this problem.

The feedback element K_B is derived next. The block diagram shown below relating displacement to flow is drawn from the elements in the bottom of Figure 1.

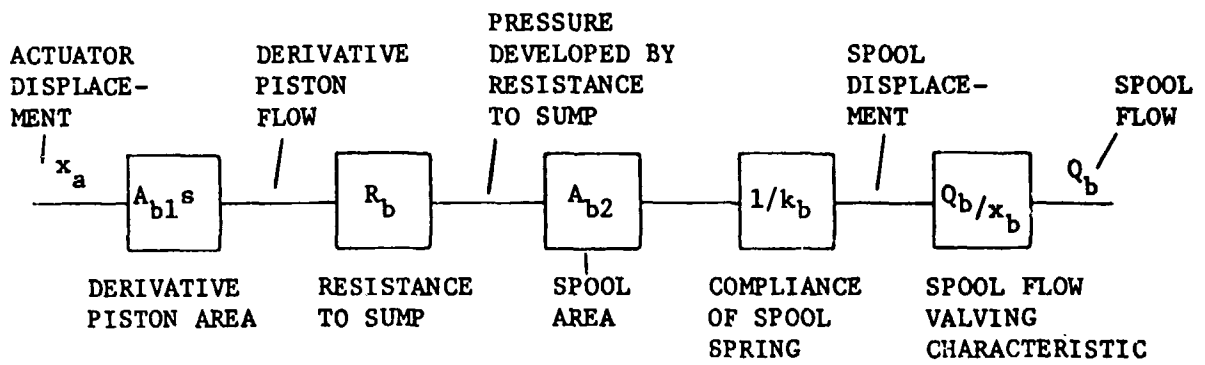

The above diagram reduces to:

$$\frac{Q_b}{x_a} = \left(\frac{A_{b1} \cdot A_{b2} \, R_b}{k_b} \cdot \frac{Q_b}{x_b} \right) s = K_B s \qquad (2)$$

Reducing the inner loop of the block diagram of Figure 2 results in Figure 3.

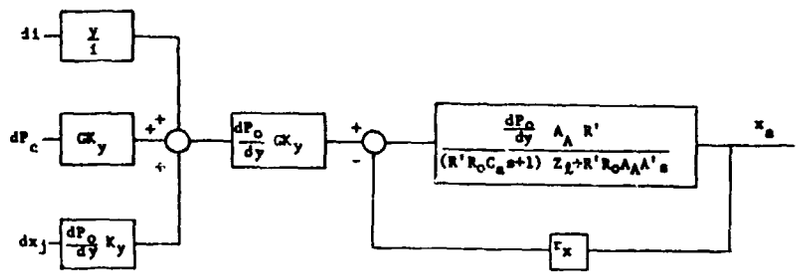

where

$$A' = A_A - K_B$$

$$R' = R_\ell / (R_\ell + R_o)$$

FIGURE 3. SERVOVALVE BLOCK DIAGRAM REDUCTION

SAMPLE CALCULATIONS

In Figure 3, there are endless variations of parameters which may be analyzed, but a representative case will be evaluated first to indicate the bandwidth degradation when the driving amplifier is a low-leakage, high-impedance element. This will be followed by design calculations using the positive derivative feedback to provide the proper damping in the inner loop. From Figure 3, inclusion of a general quadratic form for the load (Z_ℓ) in the characteristic function of the reduced inner loop yields

$$(R'R_oC_as + 1)(Ms^2 + Bs + K) + R'R_oA_AA's \qquad (3)$$

where

M is load mass, lb sec^2/in.

B is load viscous damping, lb sec/in.

K is load spring rate, lb/in.

The term A' is defined as $A_A - K_B$. Before examining the effect of K_B, first consider the two cases of a low-impedance driver and a high-impedance driver element alone (i.e., let $K_B = 0$ for the following discussion).

If a low-impedance driving amplifier is used, then $R_\ell >> R_o$, and R' approaches unity. In this case, if the actuator volume is small, the $R_o C_a$ time constant becomes negligible when compared to the load dynamics, and expression (3) becomes

$$Ms^2 + (B + R_o A_A^2)s + K \qquad (4)$$

The swept volume of the moving actuator piston provides additional damping which is usually desirable in servo loops. This case is similar to a pressure controlled servovalve in which the valve droop essentially shunts the high resistance leakage path. This provides damping. However, this is at the expense of load stiffness and flow leakage. Disturbance forces on the load can result in pressure feedback that allows flow transfer so that the load can move. In addition, a low R_o implies a large driving amplifier and thus, high flow leakage. This last characteristic is usually a reason that hydrofluidic amplifiers have difficulty competing with closed-centered valves.

In the other extreme, if a very high impedance driving amplifier were used, R_o would be greater than R_ℓ and R' approaches $\frac{R_\ell}{R_o}$ so that the characteristic function becomes

$$(R_\ell C_a s + 1)(Ms^2 + Bs + K) + R_\ell A_A^2 s \qquad (5)$$

This solution is very stiff, but it usually has stability problems. Further, if R_o is too large, the response is dominated by the first-order lag time constant, which is

$$\tau = \frac{B}{K} + R_\ell C_a + R_\ell \frac{A_A^2}{K}$$

Of this $\frac{A_A^2}{K}$ is usually much greater than C_a, so that this term becomes the limiting element in the response. If instead of $R_o >> R_\ell$, let R_ℓ approach R_o, then the term R_ℓ in the above time constant expression becomes $R_o/2$. The time constant is cut in half, but the response is still severely limited. In servo loops this has the appearance of adding excessive damping to the

loop so that it is extremely sluggish.

The servovalve, which is the subject of this discussion, is desired to be stiff while providing a reduction of leakage flow. This implies that R_o be as large as possible. However, previous hydrofluidic servovalves have resulted in R_o being low in order to achieve acceptable system bandwidth. To determine the effect of the positive derivative feedback, the characteristic expression (3) is analyzed. This feedback is through A'.

The first case to be examined will be a spring load (Z_ℓ=K). Without mass and damping, the system block diagram (Figure 3) has the following forward transfer function,

$$\frac{x_a}{y_{sp}} = \frac{\frac{dP_o}{dy} R' \frac{A_A}{K}}{R'R_o(C_a + \frac{A_A A'}{K})s + 1} \qquad (6)$$

Assume a system having a load spring of 50 lb/in., an actuator area of 0.2 $in.^2$, and a stroke of 0.2 in. If this system is driven by a 0.01 x 0.01 in. power nozzle at 2,000 psi supply pressure (resulting in output impedance of 4,000 psi/cis) and $A'=A_A$, the preceding transfer function would give a bandwidth of less than 0.1 Hz. If the positive feedback $K_B s$ is introduced to the extent that A'=0 (that is it exactly equals the valve damping, $A_A s$, which is the result of actuator displacement), the bandwidth exceeds 77 Hz. To achieve this increased bandwidth by increasing element size without the positive feedback, a much larger element flow would be required. In fact, the flow would have to be increased by a factor of 885 and the assumed 0.01 x 0.01 in. power nozzle would have to be enlarged to 0.3 x 0.3 in.

The servovalve response characteristics for selected values of R_o can be determined by setting expression (3) equal to zero and solving the resulting equation. For R_o = 4,000 psi/cis the equation factors (with A'/A_A = 1) into a low-frequency lag and a high-frequency quadratic that is considerably underdamped. As a result, a designer with a time constant equal to $(77.7 \text{ Hz})^{-1}$ coupled directly to a second-order load with a natural frequency of 100 Hz and a damping ratio of 0.5 obtains an inner loop solution

that is a low-frequency lag at 0.089 Hz and a second-order resonance at 2947 Hz with a damping ratio of 0.03. As far as the designer is concerned, this system can be characterized by the low frequency lag alone. However, in most designs this lag is unacceptable because it limits bandwidth. The designer then attempts to increase the system bandwidth by reducing the driver amplifier output resistance, R_o. This increase in element size increases leakage flow drain on the system. For no positive derivative feedback ($A'/A_A = 1$), the effect of reducing R_o can be examined. The roots for R_o = 4,000, 400, and 40 psi/cis with the 100 Hz load natural frequency are listed below to illustrate the reduction in the amplifier output impedance required to significantly increase the system bandwidth.

TABLE 1. OUTPUT IMPEDANCE EFFECT ON BANDWIDTH

Output Resistance, R_o (psi/cis)	Lag Frequency (Hz)	Resonance (Hz)	Damping Ratio
4,000	0.089	2947	0.03
400	0.890	2961	0.15
40	8.200	3061	1.28

The calculations show that to increase the system bandwidth to 8.2 Hz requires 100 times more leakage flow than the baseline example. This, in many cases, is not available to the system designer. Before examining the effect of positive feedback to achieve acceptable system bandwidth without an unacceptable flow penalty, the effect of load natural frequency on these factors can also be examined. To illustrate this, the effect of reducing R_o is listed for a load natural frequency of 10 Hz rather than 100 Hz as in the previous example.

TABLE 2. OUTPUT IMPEDANCE EFFECT ON BANDWIDTH

R_o (psi/cis)	Lag Frequency (Hz)	Resonance (Hz)	Damping Ratio
4,000	0.00089	2963	0.014
400	0.00890	2946	0.130
40	0.08800	2958	1.310

As can be seen, the lag break limits the bandwidth even more severely in this example of load natural frequency at 10 Hz. Even accepting the high flow leakage associated with R_o = 40 does not provide adequate system bandwidth.

The conventional solution of reducing the driver amplifier's output resistance does not offer any hope of achieving the system response within a flow budget; as an alternative, the use of positive derivative feedback is examined. The results of solving for the roots as A'/A_A is varied from 1 to 0 are shown in Figure 4. This figure considers the load natural frequency of 100 Hz with a damping ratio of 0.5. Three different driver amplifier output resistances are shown: the baseline case R_o = 4,000 psi/cis, R_o = 400 psi/cis, and a higher output resistance case R_o = 4,000 psi/cis. The figure contains two parts; the lag frequency is shown on the lower part and the second-order resonance on the upper part. For A'/A_A = 1, R_o = 4000 psi/cis (middle curve), the lag frequency of 0.089 Hz is shown as given earlier. At the extreme top of the figure at the same A'/A_A value the second-order resonance is given. As A'/A_A is reduced, the lag frequency increases and the load resonance decreases until at A'/A_A = 0.01 the lag frequency is 8 Hz and the load resonance is 350 Hz.

The utility of the positive feedback method of extending the bandwidth without incurring a significant flow penalty can be illustrated by assuming that the bandwidth afforded by reducing R_o from 4,000 to 400 is adequate for this system application. If the designer achieved the necessary system bandwidth by accepting the tenfold flow leakage, then the system inner loop would be characterized by a lag at 0.89 Hz and a resonance at about 2950 Hz with a damping ratio of 0.15. The system bandwidth is governed by the lag at 0.89 Hz. This same lag could be obtained with output resistance equal to 4,000 psi/cis if A'/A_A were reduced to about 0.1. The system would then be characterized by the lag at 0.89 Hz and a resonance at 942 Hz with a damping ratio of 0.09. However, in this case the flow leakage would be one tenth of the former. Since the load resonance appears so far out in frequency it makes little difference whether it resonates at 1,000 or 3,000 Hz for the modeling does not extend to these frequencies, nor will the elements respond at these frequencies.

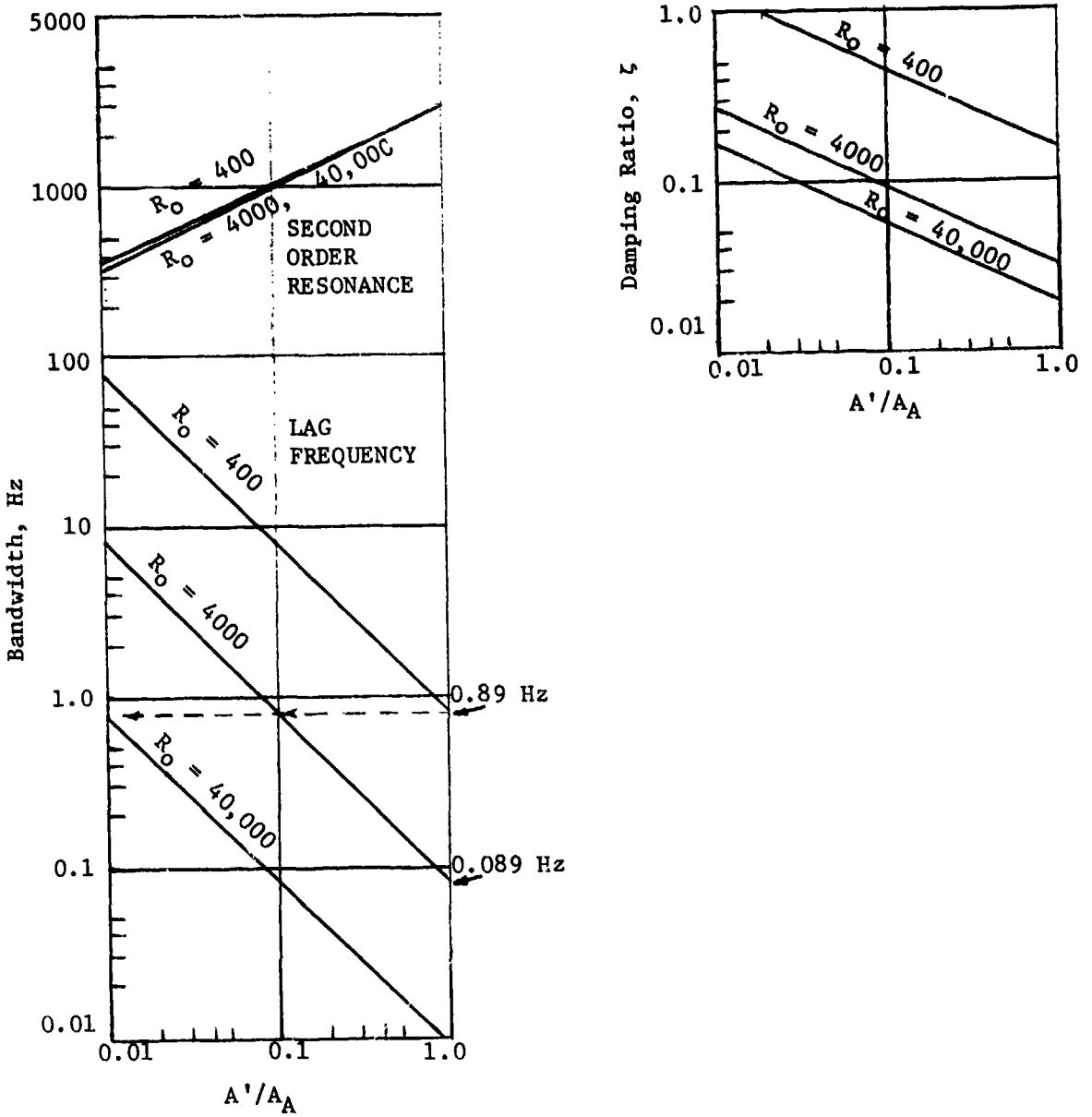

FIGURE 4. BANDWIDTH AND DAMPING RATIO

The system bandwidth can be extended to 77.7 Hz for the example given if A'/A_A is reduced to zero. However, in the earlier example the system inner loop appeared as a simple lag, which is very easy to use with a position control loop for the load. If the bandwidth is extended to the maximum, this simple inner loop solution becomes third order and little bandwidth may be gained after the compensation is developed for the tight position control loop. The inner loop solution resulting in a simple lag is more practical.

Using Figure 4, note that the 0.89 Hz bandwidth could also be achieved with the higher output resistance R_o = 40,000 psi/cis by reducing A'/A_A to 0.01. This results in a system lag frequency of 0.89 Hz and a resonance at 300 Hz with a damping ratio of 0.18. Since there is considerable separation between the lag and the resonance, this inner loop can still be characterized by a simple lag at 0.89 Hz.

The penalty in achieving this system bandwidth without increased flow leakage is the requirement that the ratio A'/A_A must be controlled with sufficient accuracy to obtain these results. This, of course, complicates the system, but advantages of achieving the bandwidth with a low cost derivative spool feedback appear to be more than worth the additional functional element.

In the design, the magnitude of A'/A_A may be controlled by using the damping adjustment shown at the bottom of Figure 1. This valve controls the magnitude of the pressure developed from a given load displacement rate. By adjusting this valve the system lag can be changed during operation to fine tune the control/load system performance. This capability alone makes the addition of this extra functional element worthwhile.

Although the plots in Figure 4 do not extend to values of A'/A_A less than 0.01, the solution of the cubic characteristic shows that the lag frequency continues to increase to higher frequencies and the second-order resonance continues to decrease until the damping becomes negative. That is, a root appears in the right half of the complex plane. This root occurs at small negative magnitudes of A'/A_A for the example calculated. This result can be intuitively expected if too much positive derivative feedback

is used. An unstable system will then result. It is suggested that this technique be limited to those cases where adequate system performance can be achieved with positive values of A'/A_A and where the system can still be characterized by a simple lag. This of course precludes making the servovalve an integrator. From the calculations it appears as though a factor of ten increase in bandwidth can be achieved without any stability problems by using the positive derivative feedback.

SERVOVALVE DESIGN

The sample calculations of the preceding section illustrate some of the trade-offs involved in achieving servovalve performance objectives through the use of positive derivative feedback. In order to design a servovalve for a set of specific objectives, the ranges of parameter variations must be reduced to manageable dimensions. The approach followed in this program has been to fix as many parameters as possible at reasonable values so that the remaining parameters may be determined by calculation and/or experiment. To do this the following performance objectives were set. These objectives are based on the Black Hawk specification.

PERFORMANCE OBJECTIVES

1. The servovalve shall accept both hydraulic pressure and electrical input control signals.
2. The valve shall be capable of driving a hydraulic actuator and associated spring/mass load with the following limitations:
   Stroke: $\pm$ 0.2 in.
   Spring rate: 0 to 100 lb/in.
   Mass (including actuator piston): 0.001 lb sec^2/in.
   Piston area: 0.200 $in.^2$
3. Bandwidth of the combined servovalve and actuator shall be less than 3 dB down at 3 Hz.
4. Dynamic response shall be achieved by use of positive derivative feedback.
5. Actuator piston position shall be controlled by direct feedback of position to the driving amplifier output jet.

HARDWARE IMPLEMENTATION

The contract servovalve specification calls for a unit capable of physically interfacing with a Black Hawk SAS actuator assembly. Since no Black Hawk actuator was available, the decision was made to design a breadboard representative of the Black Hawk servovalve/actuator system, using an available actuator to simulate that of the Black Hawk system. This design permits demonstration of the principles involved without the constraints of high-density packaging.

The breadboard arrangement consists of discrete components (amplifiers, valves, feedback mechanisms) interconnected by hydraulic tubing and mechanical links. This arrangement permits flexibility of measurement and adjustment at many intermediate points during development and testing of the system.

To maximize the use of available time and funding, existing components were used whenever possible. Figures 5 and 6 show the breadboard arrangement. The components are described below.

Actuator - The design of an actuator was not within the scope of this program. However, an actuator built for a previous AVRADCOM investigation[1] (shown in Figures 5 and 7) was available.

Derivative Piston Assembly - This is shown as item 1 on Figure 5. Essentially, this unit converts actuator piston velocity into hydraulic pressure which drives the spool valve. A resistor valve connected to ground, item 4, is mounted on the assembly.

---

1 Hedeen, James O., INVESTIGATION OF A LOW-COST SERVOACTUATOR FOR HYSAS, Honeywell, Inc.; USARTL Technical Report 78-30, Applied Technology Laboratory, U. S. Army Research and Technology Laboratories (AVRADCOM), Fort Eustis, Virginia, July 1978, AD A059188.

Spool Valve - A spool valve from an existing servovalve was mounted in a housing machined specifically for this breadboard. The spool and housing assembly, item 2 of Figure 5, permits positive feedback flow to the actuator in response to the derivative piston demand. An adjustment screw, item 3, permits centering the spool. Pressure (P_b) developed by the derivative piston displaces the spool valve, admitting flow (Q_b) to the actuator. The relationship between P_b and Q_b was determined by test and is shown for two values of spool supply pressure (P_s=100 psi and 250 psi) in the upper part of Figure 8. Spool valve flow, Q_b, is shown as a function of spool displacement, x_b, for several values of P_s in the lower part of Figure 8.

Fluid Amplifiers - Two fluid amplifiers are used. Both amplifiers are TriTec A1-12 amplifiers that have been modified so that the tip of the fluid stream splitter can be moved laterally in the fluid stream. In the control amplifier (item 7 of Figure 5), the splitter is driven by an electrical torque motor (item 8) via a rod (item 12). In the second-stage amplifier (item 6), the moveable splitter is driven by a feedback bar (item 9) attached to the actuator piston. Details of the moveable splitter portion of the amplifier are shown in Figures 6A and 6C. The amplifiers are comprised of unbonded laminates held between removable cover plates to permit change of aspect ratio as required during testing. The amplifier laminate plan form is shown in Figure 9.

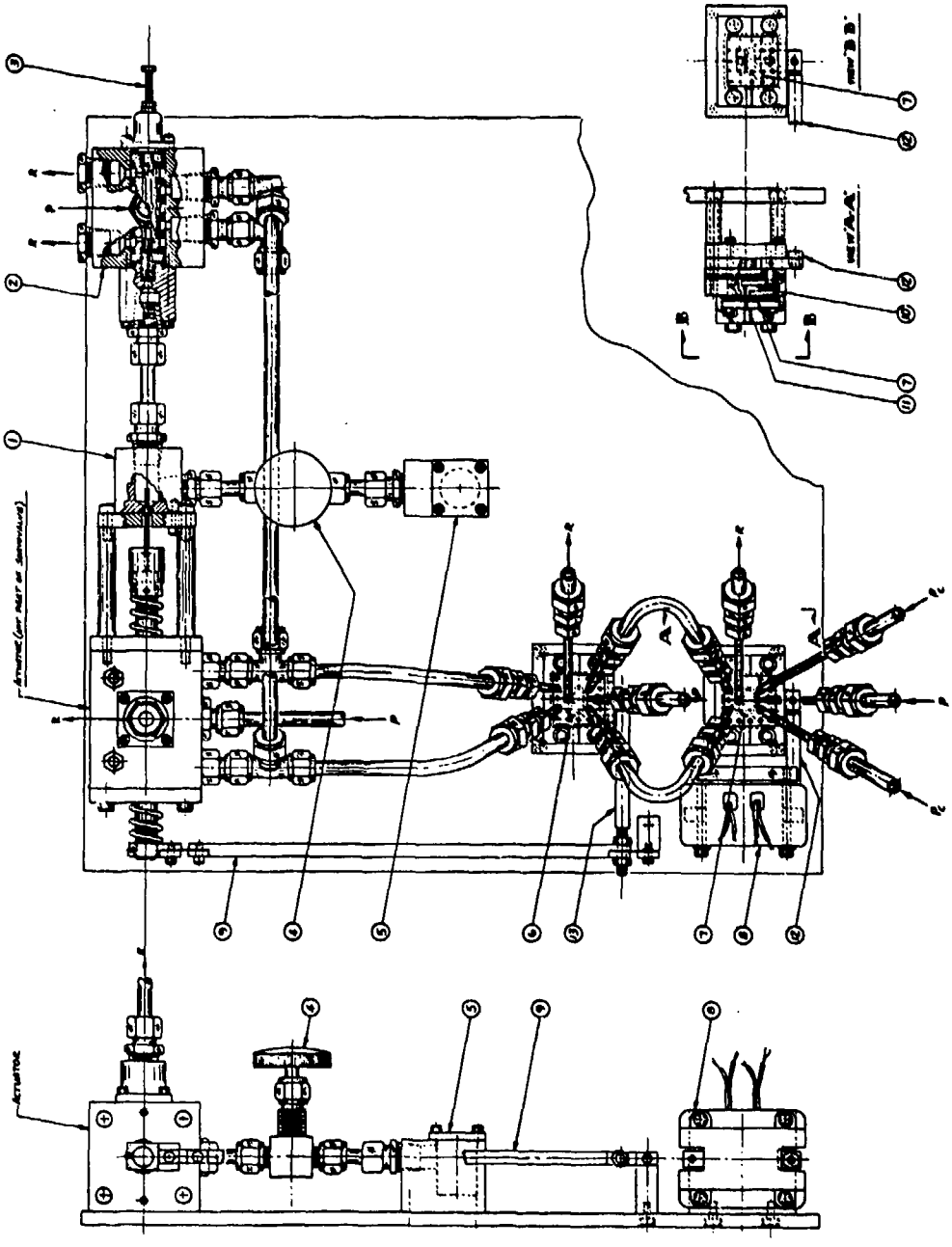

FIGURE 5. SERVOVALVE BREADBOARD ARRANGEMENT

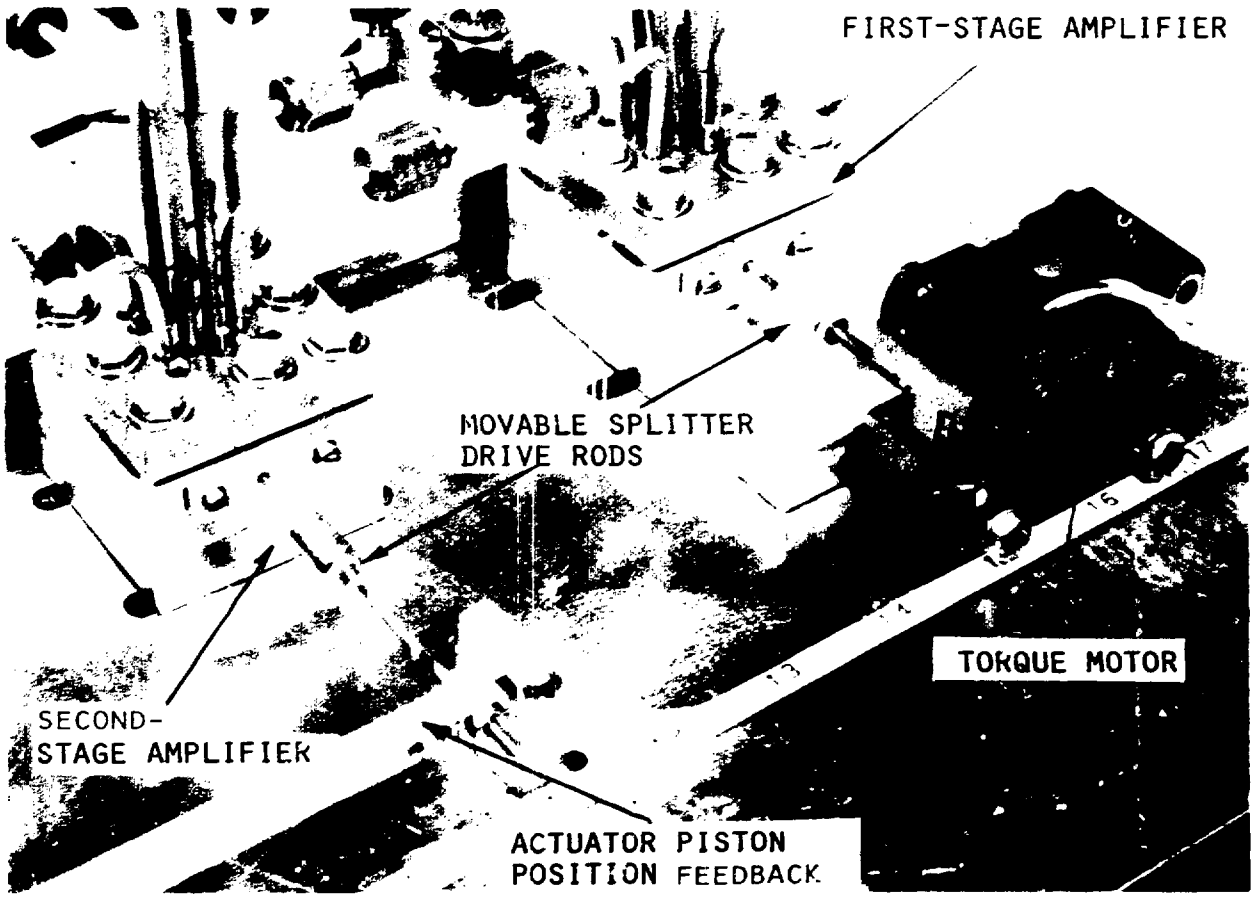

FIGURE 6A. SERVOVALVE AMPLIFIERS AND TORQUE MOTOR

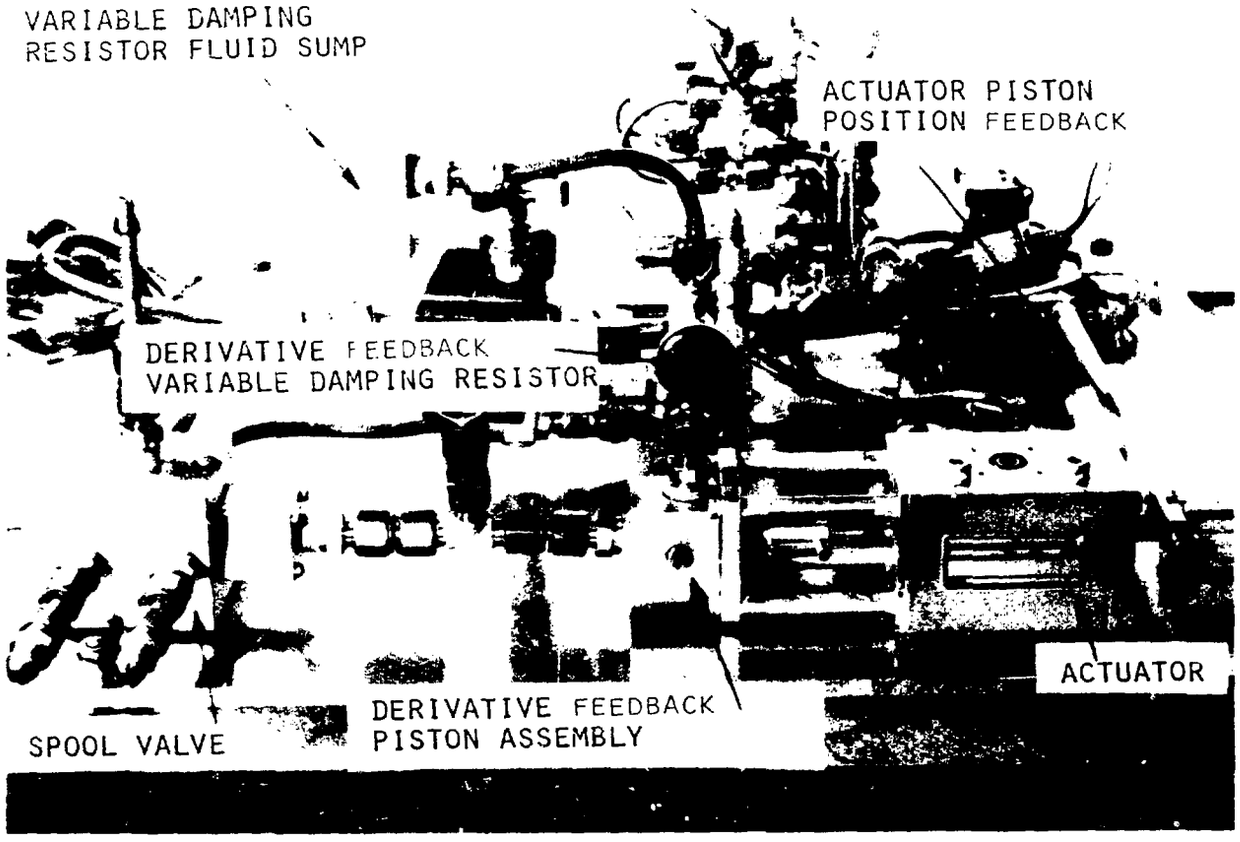

FIGURE 6B. SERVOVALVE DERIVATIVE FEEDBACK MECHANISM

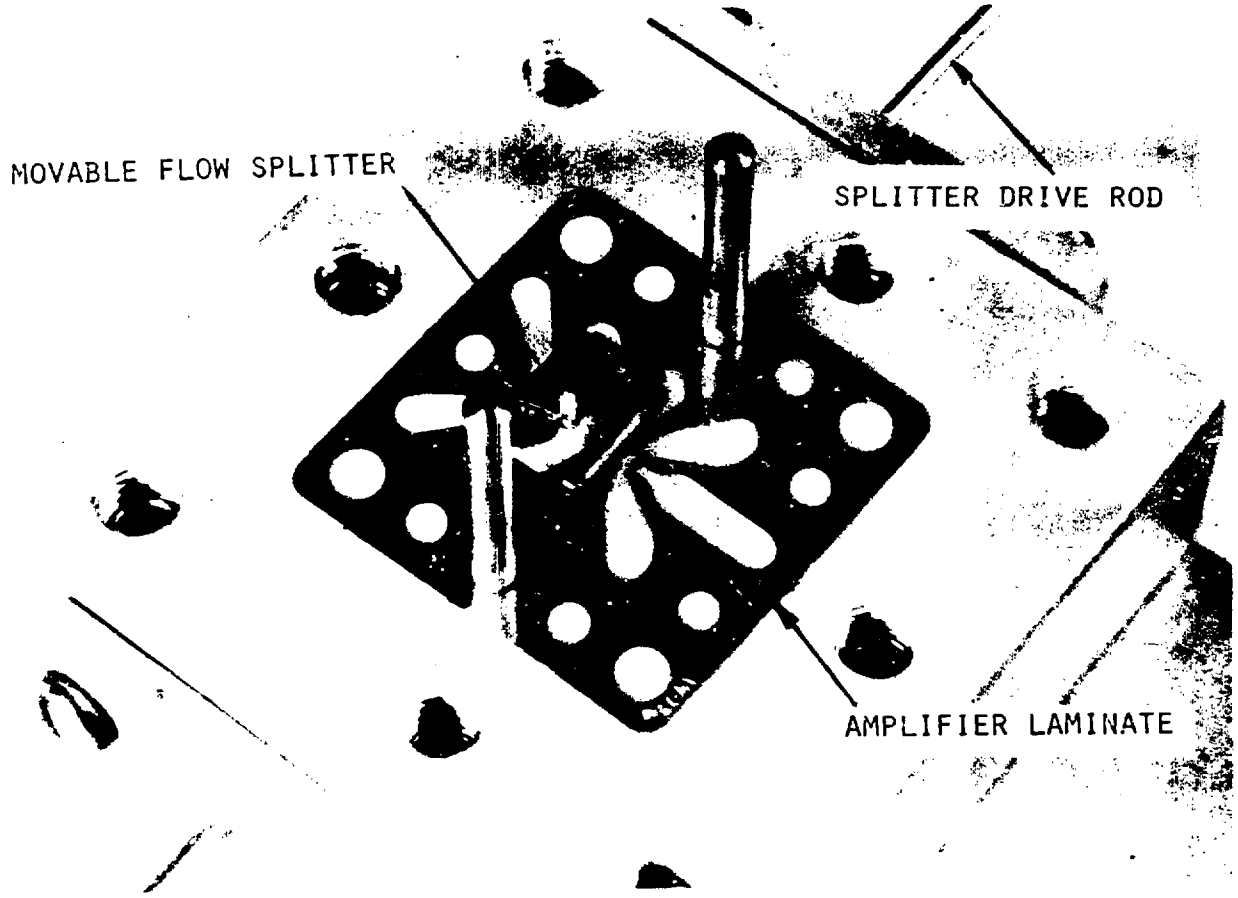

FIGURE 6C. AMPLIFIER BASE DETAILS

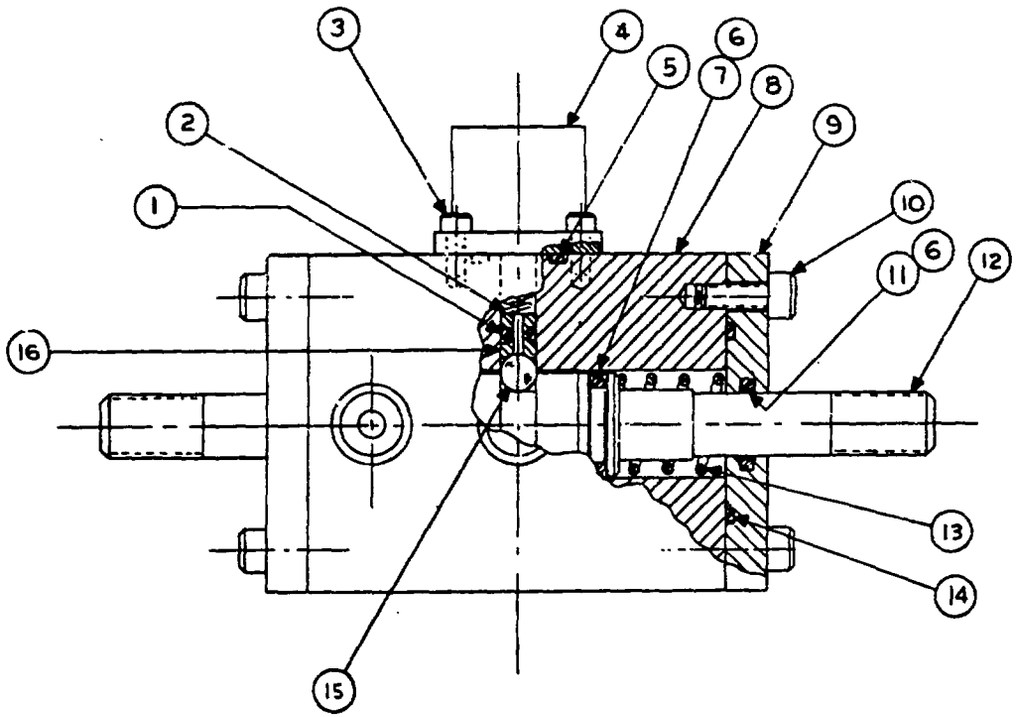

1 O-RING
2 SPRING, LOCKING
3 SCREW, SOCKET HEAD
4 BOSS, RETURN
5 O-RING
6 O-RING
7 GLYD RING
8 BODY, CYLINDER
9 PLATE, END
10 SCREW, SOCKET HD
11 GLYD RING
12 PISTON, CYLINDER
13 SPRING (REMOVABLE)
14 O-RING
15 BALL
16 SPOOL, LOCKING

FIGURE 7. ACTUATOR

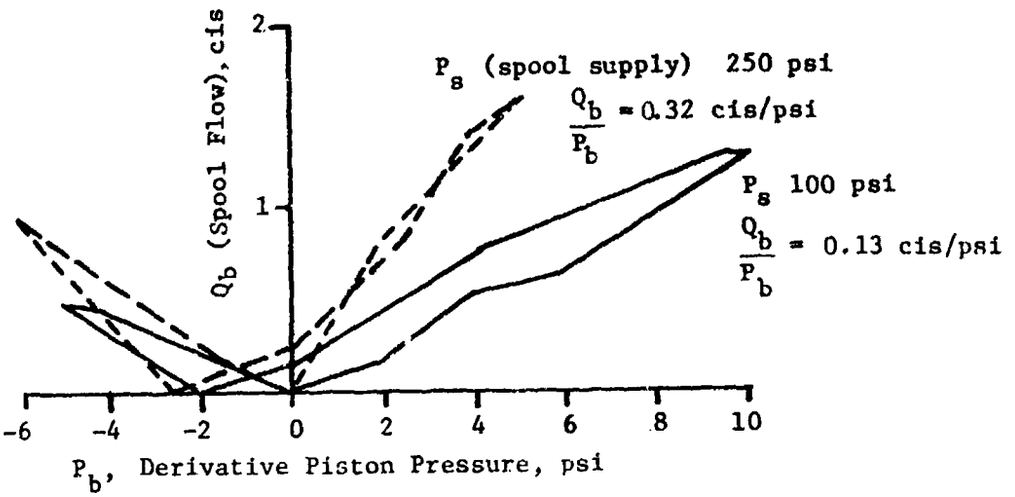

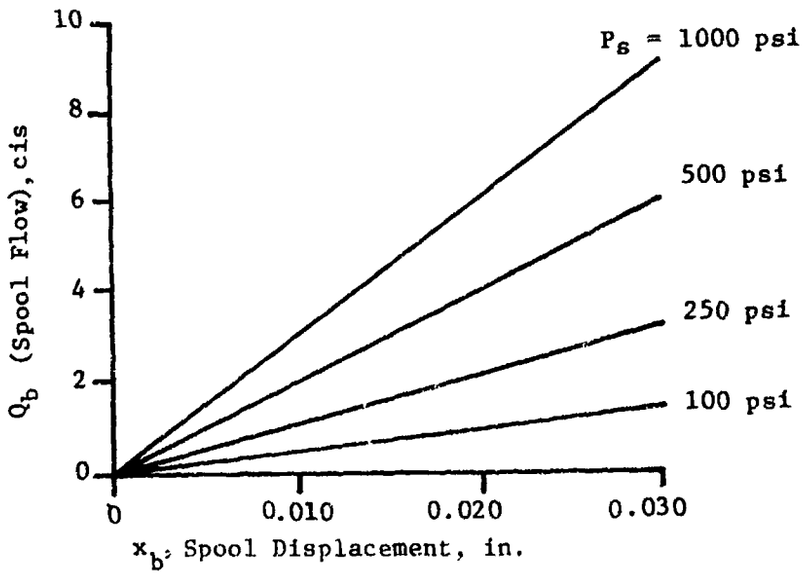

FIGURE 8. SPOOL FLOW CHARACTERISTICS

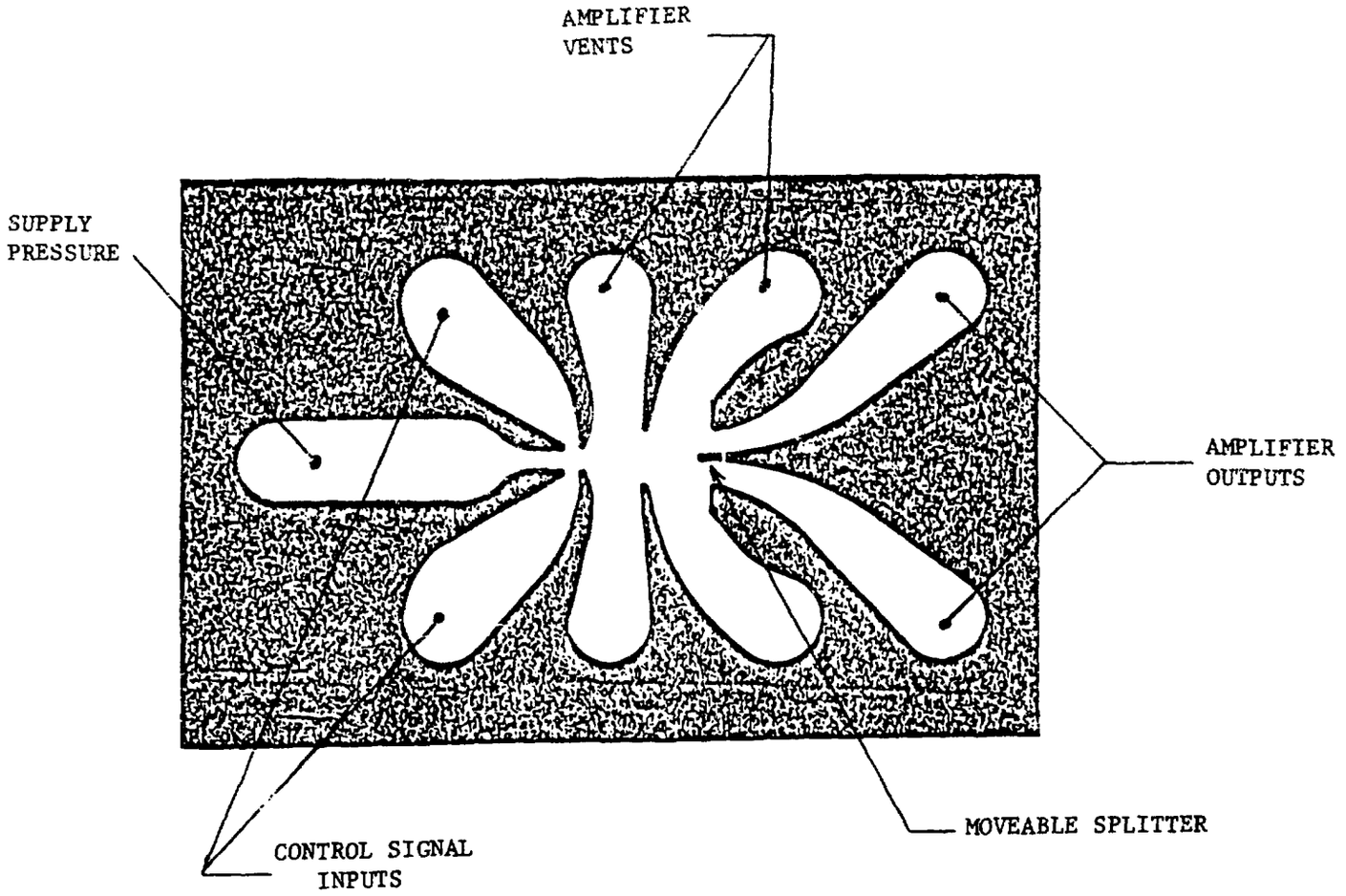

FIGURE 9. PROPORTIONAL FLUIDIC AMPLIFIER PLAN VIEW

To accomplish the performance objectives, the following initial parameter values (as defined in the Mathematical Model section) were selected:

Amplifier supply orifice, 0.020 x 0.020 in.
Supply pressure = 2000 psi
R_o = 250 psi/cis (See Figure 13)
$C_a = 4.6 \times 10^{-6}$ in.^{3}/psi
$R_\ell = 10\ R_o$
$R' = R_\ell/(R_\ell + R_o) = 0.91$
$A_A = 0.200$ in.^{2}
$A_{b1} = 1.23 \times 10^{-2}$in.^{2}
$A_{b2} = 3.08 \times 10^{-2}$in.^{2}
k_b = 5.5 lb/in.
M = 0.001 lb sec^2/i.
B = 0.1414 lb sec/in.
K = 5.0 lb/in.
r_x = 32
P_s = 500 psi
Q_b/x_b = 100 cis/in.

PERFORMANCE PREDICTIONS

Using the initial parameter values listed previously, the dynamic response of the servovalve/actuator combination is calculated by solving the inner loop characteristic equation of expression (3). By solving this equation for a range of derivative feedback values, the variation in first- and second-order response frequencies, as well as system damping, can be determined. The results are plotted in Figure 10. This figure shows a calculated lag (first-order) resonant frequency of 0.09 Hz and a second-order frequency of 475 Hz for $A'/A_A = 1$ (i.e., with no derivative feedback).

As the derivative feedback is increased to $A'/A_A = 0.015$, the lag frequency increases to 3 Hz, which is the design goal. Further increase in derivative feedback ($A'/A_A \rightarrow 0$) shows the lag frequency increasing to 8 Hz at $A'/A_A = 0.001$, two orders of magnitude higher than the lag frequency with no derivative feedback. Throughout this range the second-order resonant frequencies remain above 50 Hz, well above the performance range of the servovalve.

Based on the indicated bandwidth of Figure 10, the servovalve frequency response has been calculated for no derivative feedback (A'/A_A=1.0) and for sufficient derivative feedback (A'/A_A=0.015) to raise the lag frequency to 3 Hz (at the -3 dB level). The calculated response curves are shown in Figure 11.

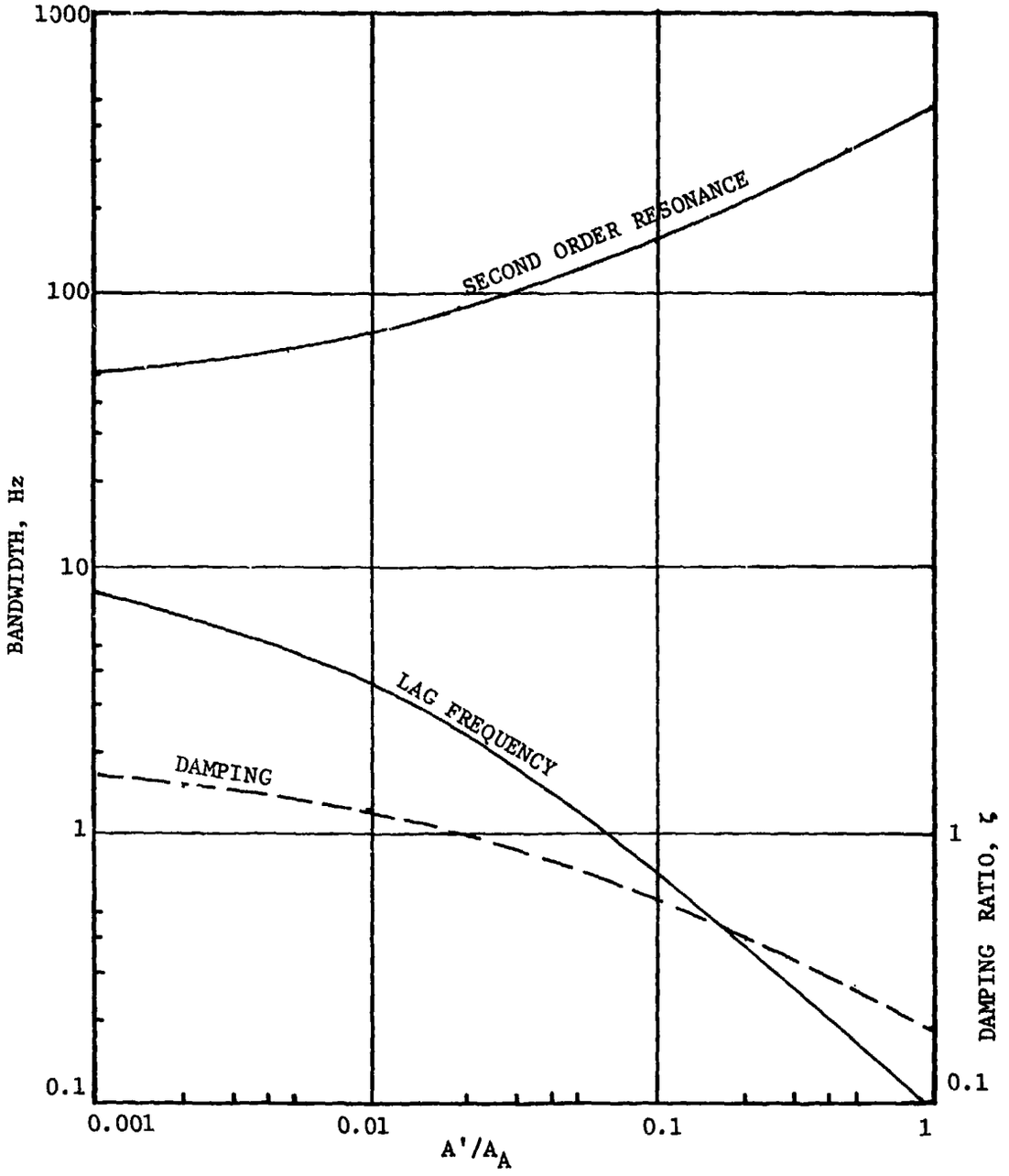

FIGURE 10. BANDWIDTH VS. DERIVATIVE FEEDBACK

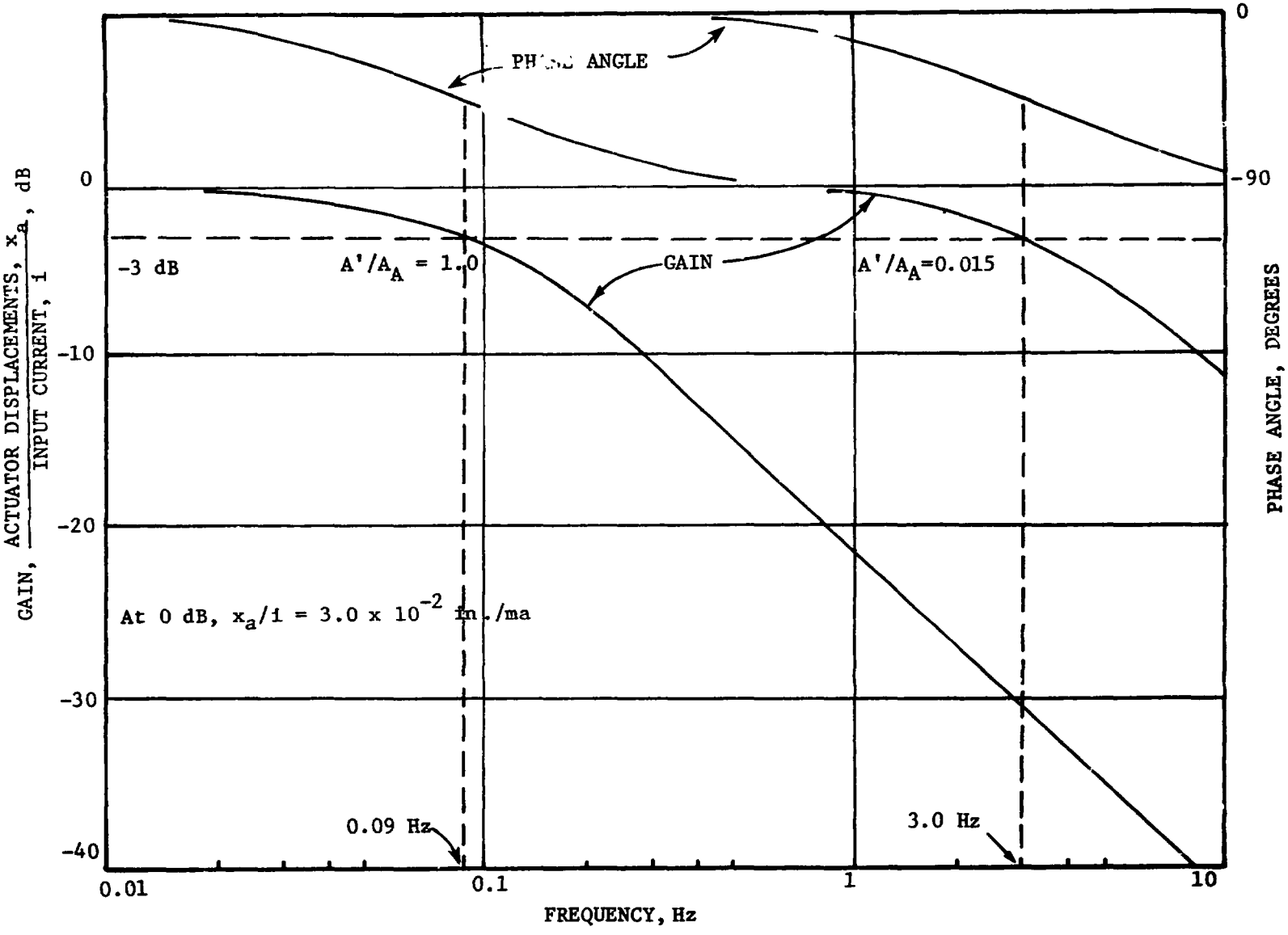

FIGURE 11. CALCULATED ACTUATOR RESPONSE

PERFORMANCE DEMONSTRATION

A test program was conducted to demonstrate concept feasibility. Component tests were conducted to determine parameter values such as spring rates and flow characteristics for use in the design calculations and performance predictions. The assembled components were then instrumented so that significant pressures, displacements, flow rates, and velocities could be measured and compared with the corresponding elements of the block diagram and math model. The math model described previously was used to compare the performance of the servovalve with the requirements of the Black Hawk specification and to show how performance could be altered by specific hardware changes.

TEST SETUP AND INSTRUMENTATION

Figure 12 is a schematic of the servovalve showing points at which measurements were taken. Pace Model KP15 transducers (0 to 500 psi) were used at locations 2, 5, and 9, and a Pace Model P3D (0 to 3000 psi) was used at location 7. Pace Model CD25 transducer indicators were used for readout. Splitter motion at points 4 and 6 was measured by Schaevitz Model E-100 LVDT's ($\pm$ 0.100 in. range) and actuator displacement was measured by a Bourns potentiometer-type transducer ($\pm$ 1 in. range). For dynamic response tests, an HP Model 3575A gain-phase meter was used. Hydraulic control and supply pressures were monitored by means of calibrated gauges.

TEST PROCEDURES

A matrix of the system tests is shown in Table 3. Five series of tests were conducted. Series I, II, and III consisted of input control signal sweeps with the actuator blocked and the derivative feedback portion of the system inoperative. Series IV was run with the actuator free to move without derivative feedback. Series V was run with derivative feedback.

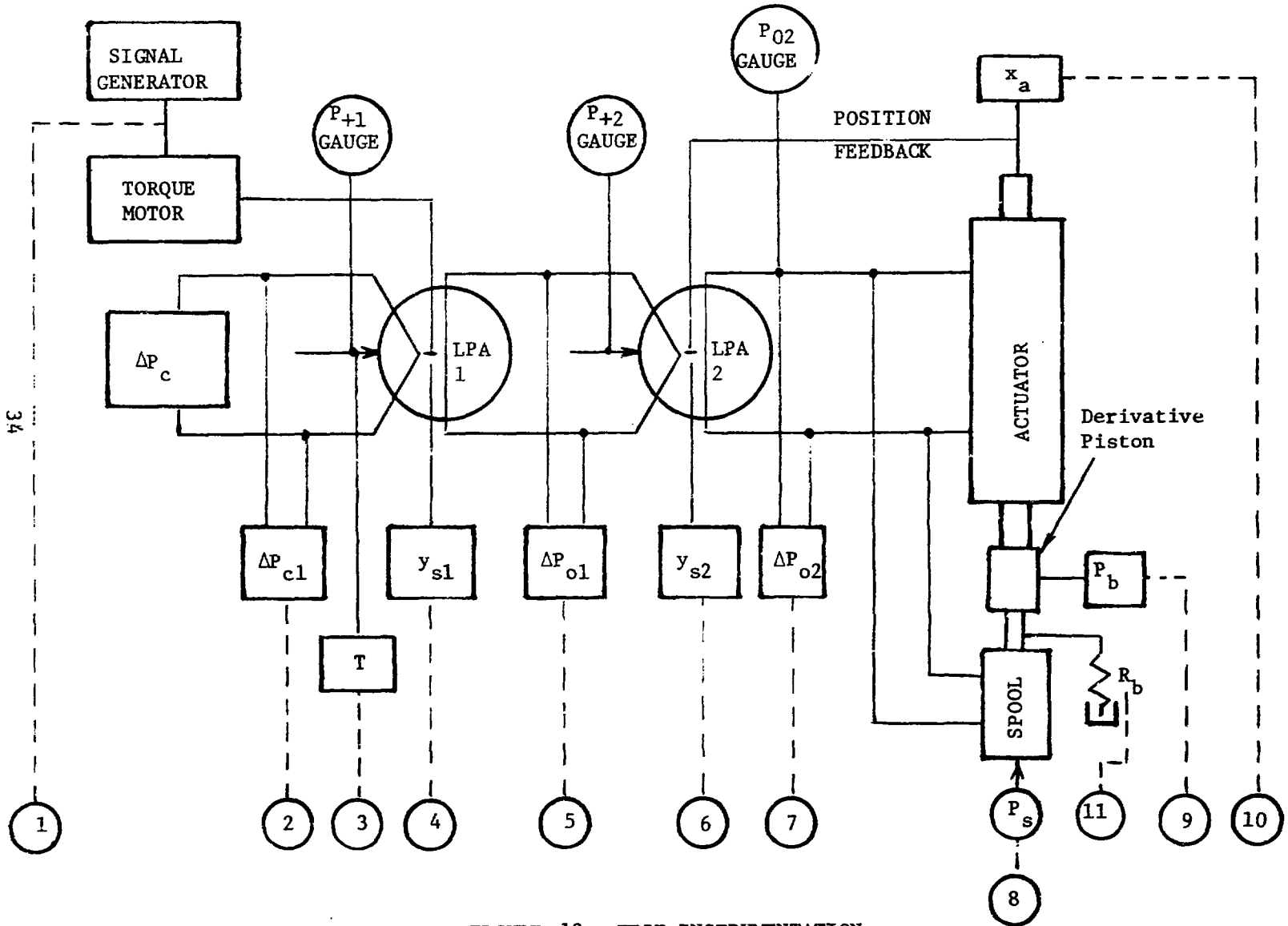

FIGURE 12. TEST INSTRUMENTATION

TABLE 3. SCHEDULE OF TESTS

PARAMETER / TEST SERIES	①(a) INPUT SIGNAL	② ΔP_{c1}	③ TEMP.	④ y_{s1}	⑤ ΔP_{o1}	⑥ y_{s2}	⑦ ΔP_{o2}	⑧ P_s SPOOL	⑨ P_b DERIV. PISTON	⑩ x_a	⑪ R_b VALVE SETTING
I	S(b)	V(c)	OUT(d)	S	OUT	S	OUT	-	-	-	-
II	V	S	OUT	V	OUT	S	OUT	-	-	-	-
III	V	S	OUT	V	OUT	S	OUT	-	-	-	-
IV	V	S	OUT	V	OUT	OUT	OUT	-	-	-	-
V	V	S	OUT	V	OUT	OUT	OUT	S	OUT	OUT	S

NOTES: a. Circled numbers keyed to instrumentation diagram, Figure 12.

b. S indicates value set at preselected levels.

c. V indicates value varied in steps or sinusoidally.

d. OUT indicates output data.

Parameters were varied during each series as follows:

Series I

ΔP_c swept

y_{s1} splitter set at selected positions

y_{s2} splitter set at selected positions

Series II

y_{s1} splitter swept by torque motor

ΔP_c set at selected levels

y_{s2} splitter set at selected positions

Series III

y_{s1} splitter sinusoidal input (signal generator driving torque motor)

ΔP_c set at 0 psid

Series IV

y_{s1} splitter sinusoidal excitation

ΔP_c set at 0 psid

Series V

y_{s1} splitter sinusoidal excitation

ΔP_c set at 0 psid

R_b and P_s (derivative feedback resistance and spool supply pressure) set at selected levels.

Tests were run with first-stage supply pressure at 400 and 500 psi, second-stage supply pressure at 1000 and 2000 psi, respectively, and system back pressure at 10 psi. Series V was run with the spool supply pressure (P_s) set at 500 psi.

RESULTS OF TESTS

The test data are presented in Figures 13-27. Figure 13 shows the amplifier output resistance (R_o) as determined by the average slopes of the output flow vs. pressure curves for the two combinations of supply pressures (P_{+1} and P_{+2}) noted on the graph. Servovalve leakage is shown in Figure 14. Figure 15 illustrates the effect of spool supply pressure (P_s) on actuator stroke (x_a) when oscillating the servovalve at a fixed frequency of 0.6 Hz. Of significance in Figure 15 is the abrupt increase in actuator stroke when spool supply pressure exceeds 700 psi, indicating the onset of instability at that pressure.

Figures 16-27 present performance data of various elements represented in the system block diagram (Figure 3). Figures 20 and 21 illustrate the hysteresis effects of actuator and splitter friction at low frequency (0.02 Hz), while Figures 22 and 23 show the reduced hysteresis when operating the servovalve at very slow speeds (approaching zero frequency). Using the performance data to determine the values of the parameters in the

block diagram, we have

1. $y/i = 0.00156$ in./milliamp, taken as the mean slope of the curve in Figure 16
2. $(GK_y)_1 = 5.18 \times 10^{-4}$ in./psid, determined from Figure 17
3. $(dP_o/dy)_1 = 3.230 \times 10^3$ psid/in., from the slope of the curve in Figure 18 for $\Delta P_c = 0$
4. $(dP_o/dy)_2 = 1.48 \times 10^4$ psid/in. from Figure 19, y-axis intersections
5. $(GK_y)_2 = 1.88 \times 10^{-4}$ in./psid from Figure 19, x-axis intersections
6. $\Delta P_{o2}/\Delta P_{o1} = 2.63$, second-stage pressure gain, mean slope of curves in Figure 19
7. $x_a/i = 0.05$ in./mA from Figure 20
8. $x_a/\Delta P_c = 0.002$ in./psid, Figure 23
9. $r_x = 0.031$, obtained from transducer voltage readouts when stroking actuator manually
10. $\Delta P_{o1}/\Delta P_c = 2.80$, first-stage pressure gain, slope of curve in Figure 24

The above parameters relate to the static or DC portion of the block diagram. The inner loop elements determine the dynamic response of the system and are best interpreted in terms of the system frequency response. Figure 25 is the frequency response of the fluidic portion of the servovalve: i.e., it relates the response of ΔP_{o2} to motion of the first-stage splitter with the actuator blocked over the frequency range of 0.5 to 30 Hz. Figure 26 shows the actuator response to input splitter motion from 0.5 to 20 Hz without derivative feedback and Figure 27 shows the actuator response over the same frequency range with derivative feedback.

DISCUSSION OF TEST RESULTS

The static, or nonfrequency dependent, elements of the math model are listed as items 1 through 10 of the preceding section. Several checks can be made to determine overall correlation among them. First, following the block diagram from the current control input to the resultant actuator motion,

$$(y/i) \times \left(\frac{dP_o}{dy}\right)_1 \times (GK_y)_2 \times \frac{1}{r_x} = \frac{x_a}{i} \tag{7}$$

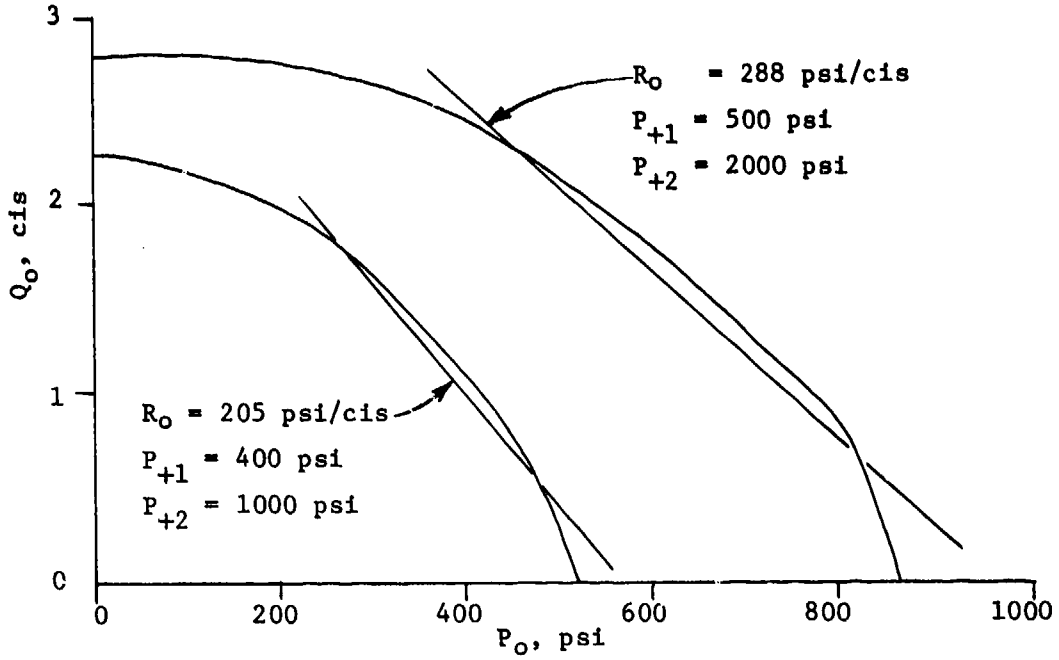

FIGURE 13. AMPLIFIER OUTPUT RESISTANCE

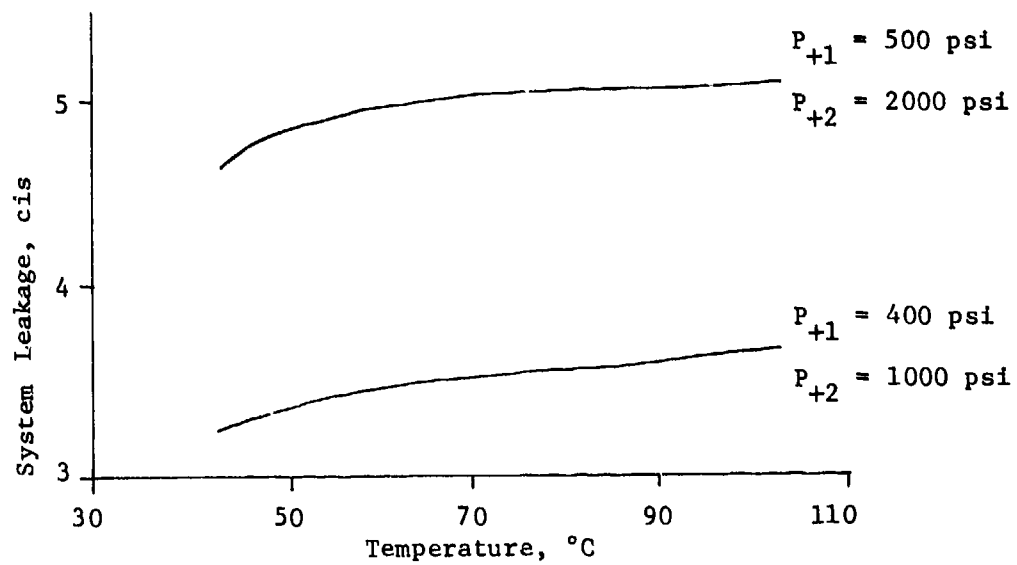

FIGURE 14. SERVOVALVE LEAKAGE

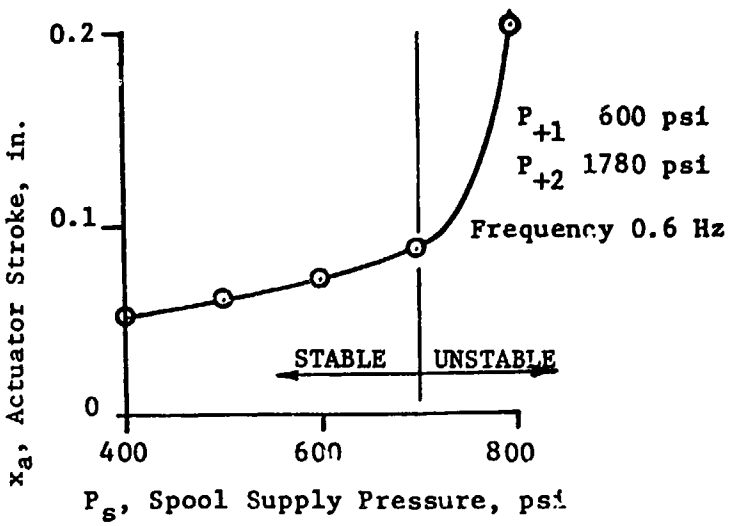

FIGURE 15. ACTUATOR STROKE VS. SPOOL SUPPLY PRESSURE WITH DERIVATIVE FEEDBACK

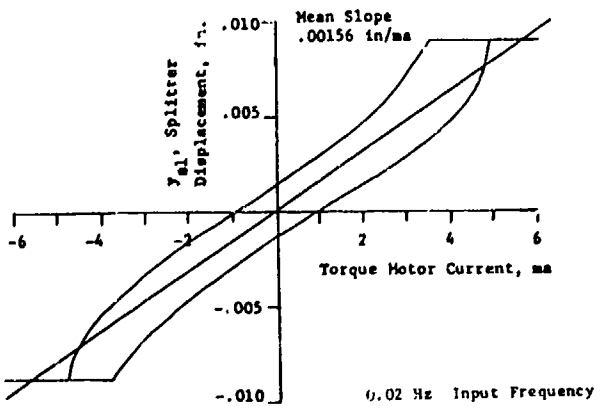

FIGURE 16. FIRST-STAGE SPLITTER RESPONSE TO INPUT CURRENT

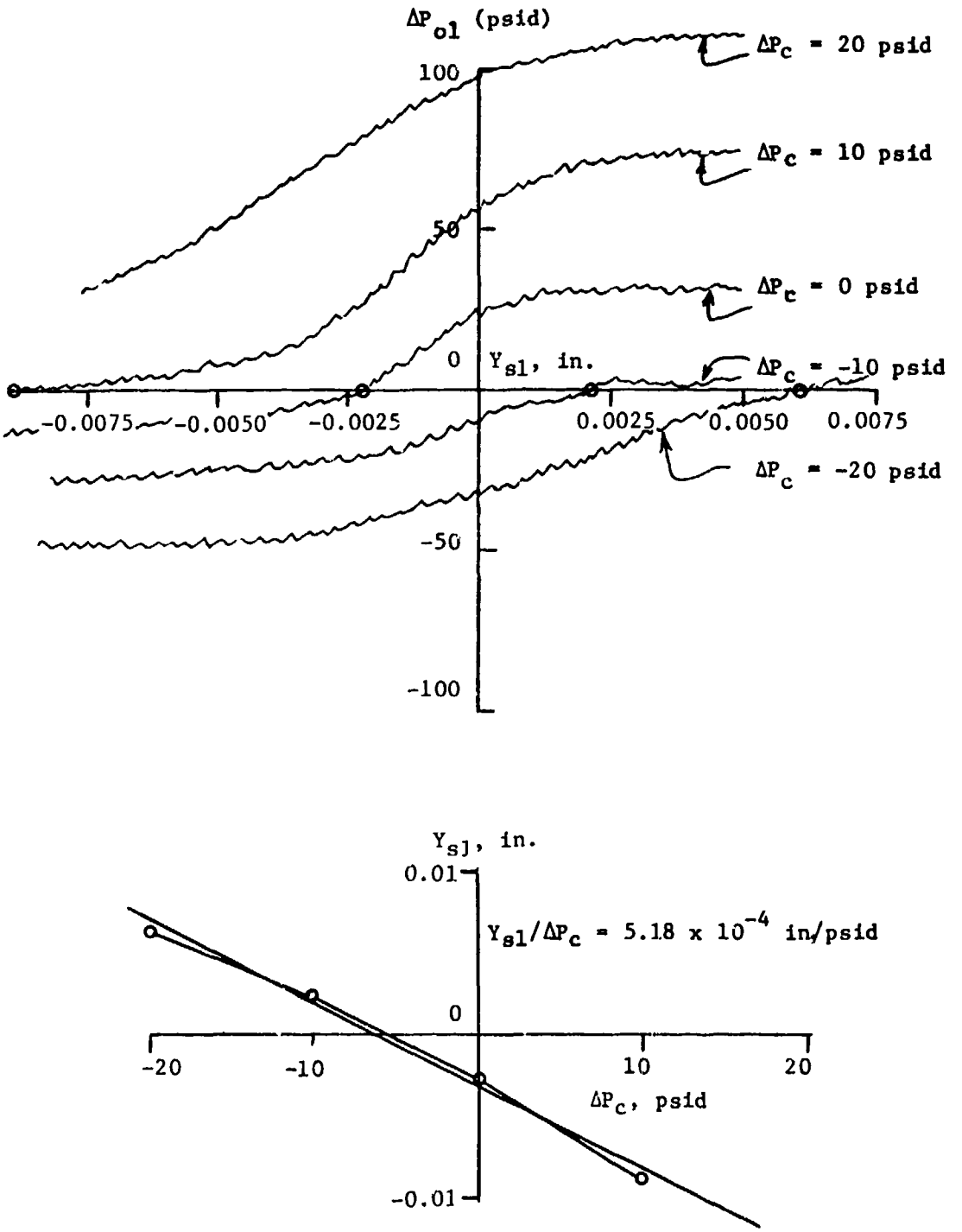

FIGURE 17. SPLITTER MOTION/ΔP_c RELATIONSHIP

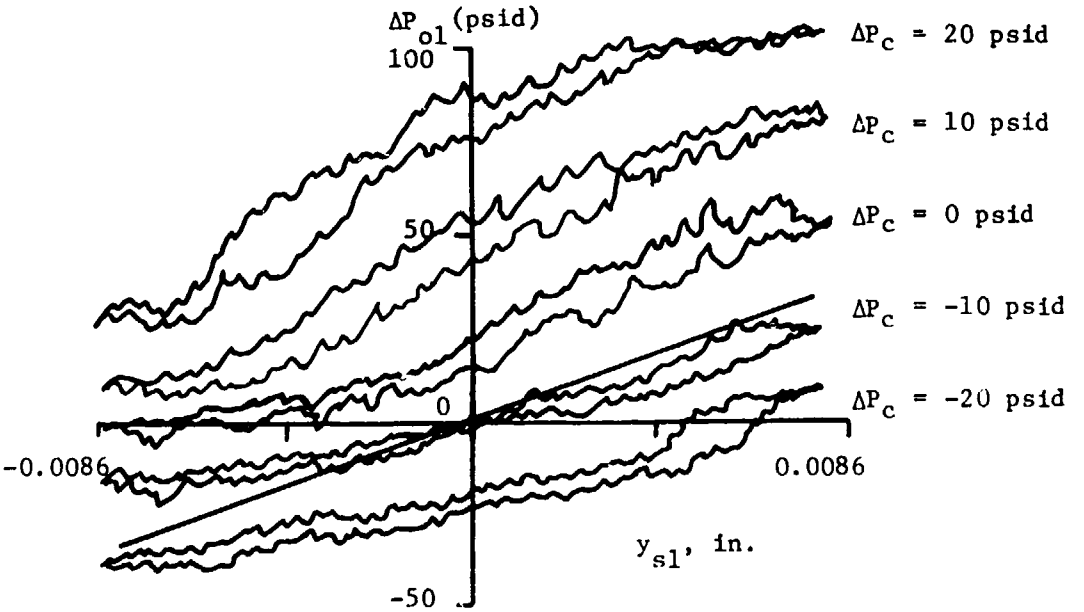

$\Delta P_{o1}/y_{s1}$ = 3230 psid/in.

FIGURE 18. ΔP_{o1} VS. y_{s1} AS A FUNCTION OF ΔP_c

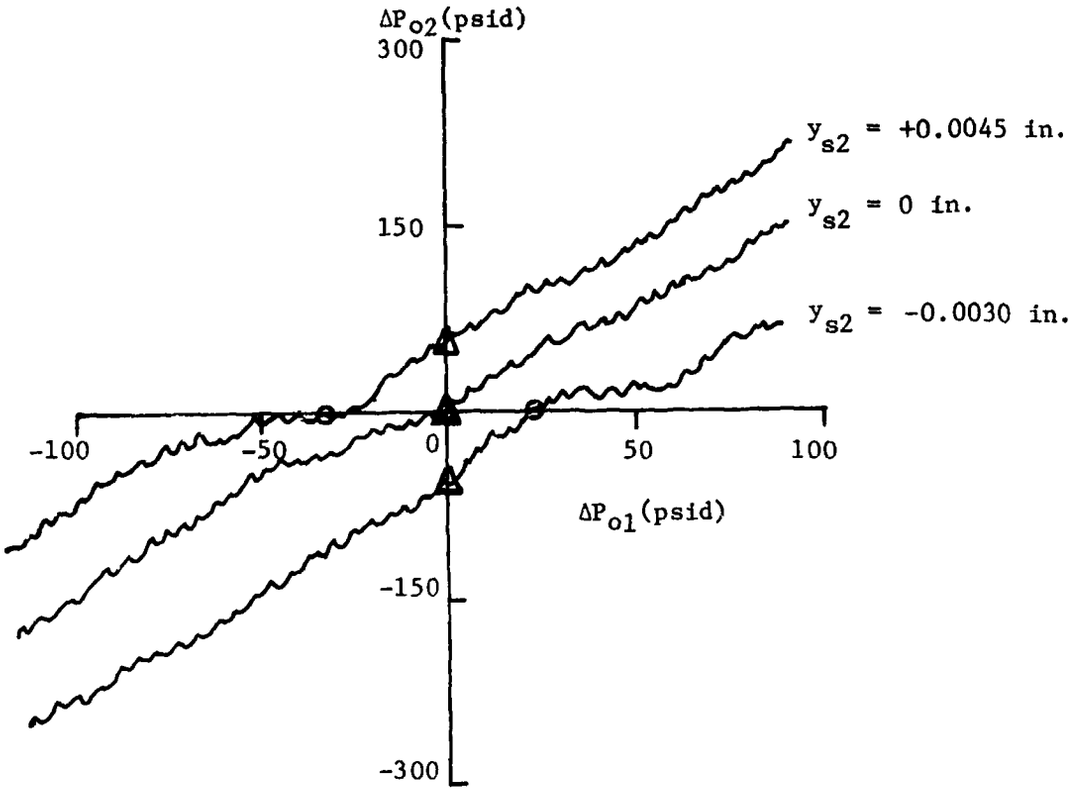

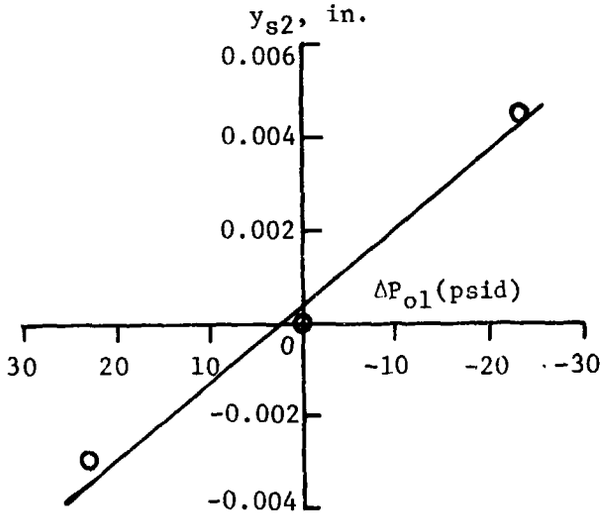

X AXIS CROSSINGS

$y_{s2}/\Delta P_{o1} = 1.88 \times 10^{-4}$ in./psid

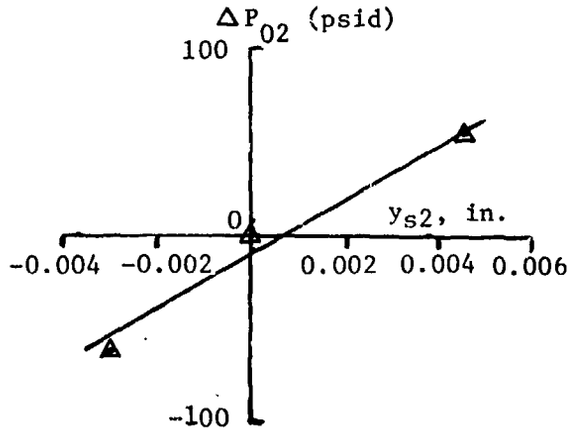

Y AXIS CROSSINGS

$\Delta P_{o2}/y_{s2} = 1.48 \times 10^{4}$ psid/in.

FIGURE 19. ΔP_{o2} VS. ΔP_{o1} AS A FUNCTION OF y_{s2}

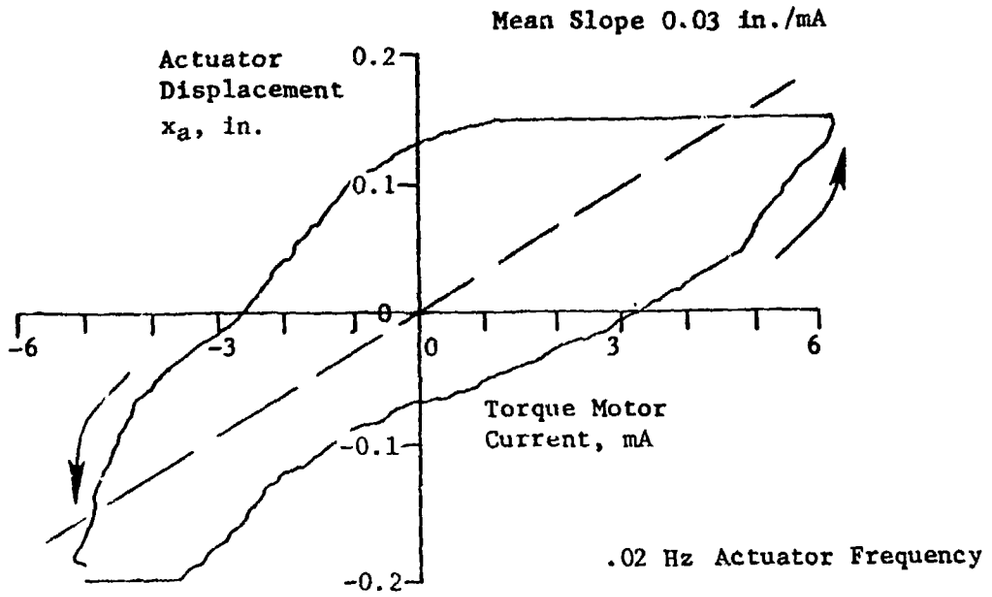

FIGURE 20. ACTUATOR MOTION VS. TORQUE MOTOR CURRENT

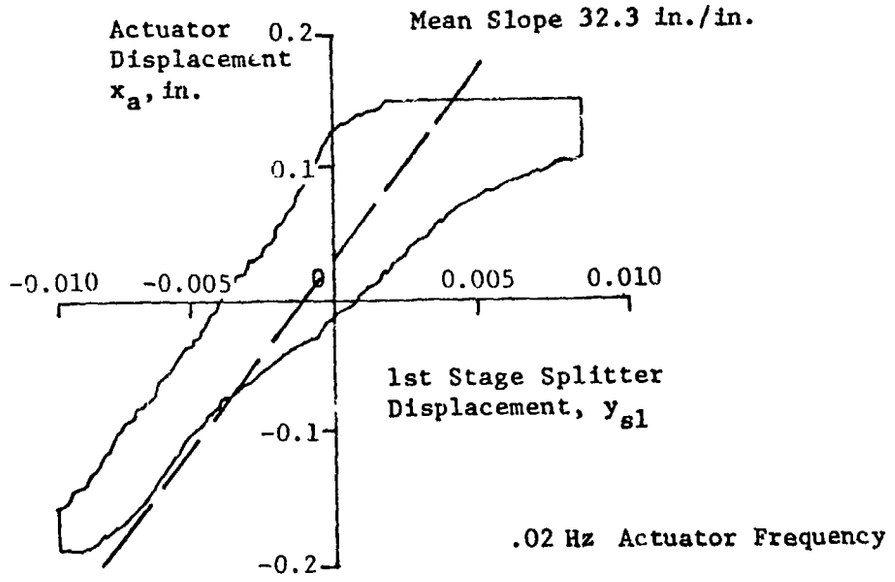

FIGURE 21. ACTUATOR MOTION VS. FIRST-STAGE SPLITTER MOTION

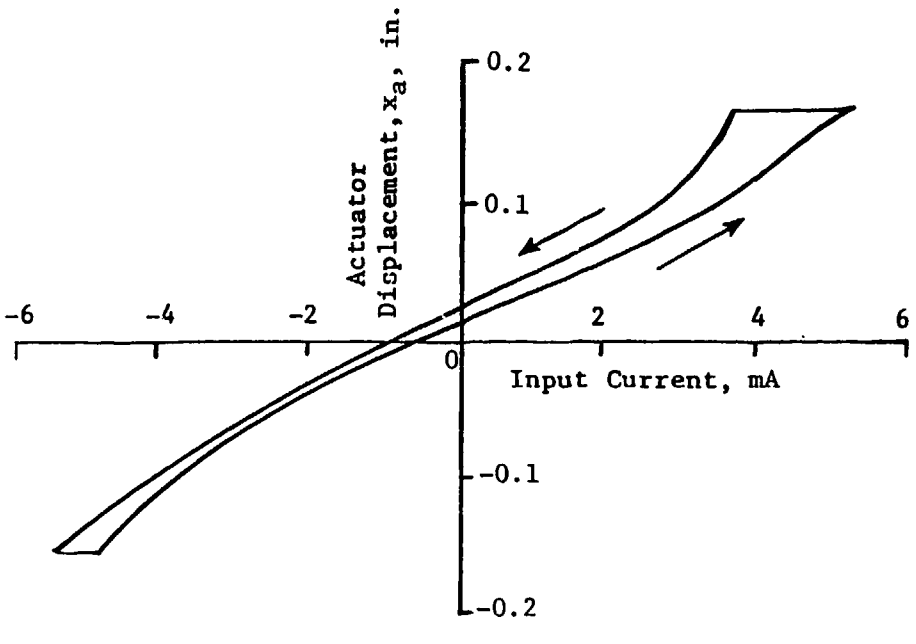

FIGURE 22. ACTUATOR DC RESPONSE TO INPUT CURRENT

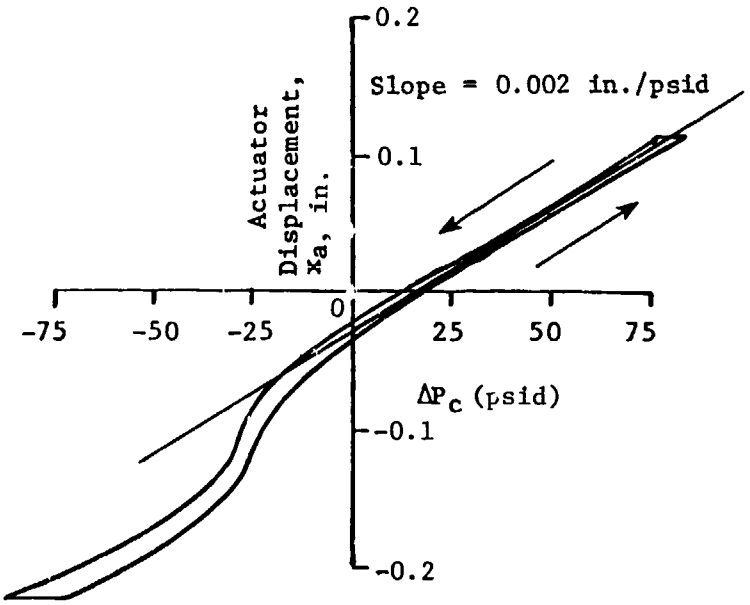

FIGURE 23. ACTUATOR DC RESPONSE TO INPUT PRESSURE

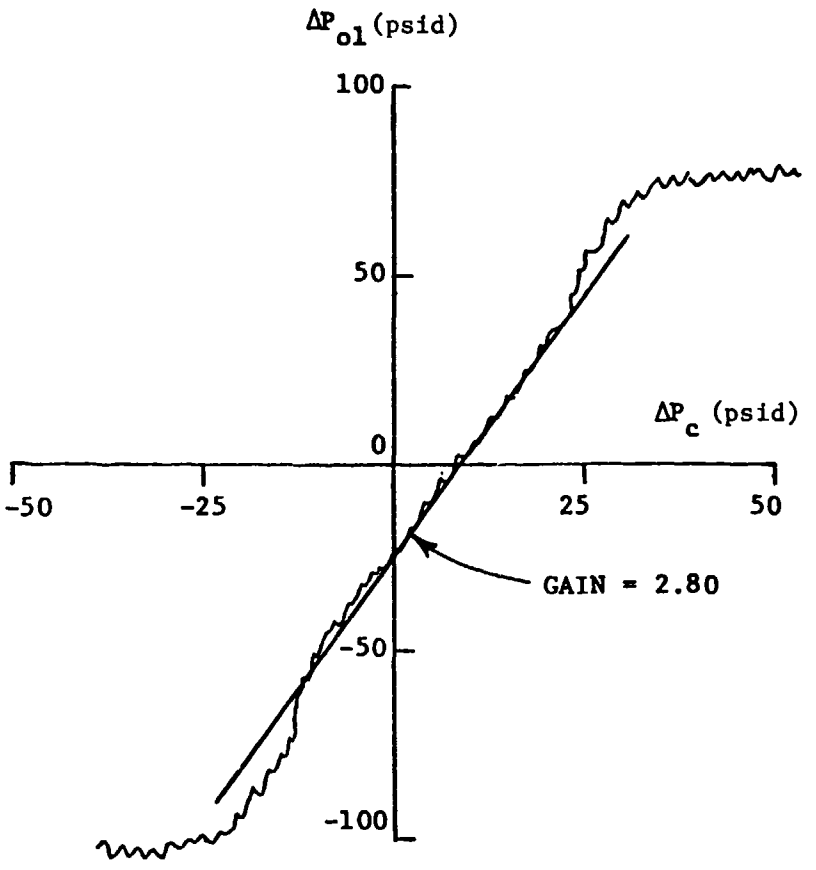

FIGURE 24. FIRST-STAGE AMPLIFIER GAIN

Substituting the above values in Equation (7),

$$x_a/i = (0.00156)(3.230 \times 10^3)(1.88 \times 10^{-4})(32) = 0.03 \text{ in./mA}$$

This calculated value is shown as the dashed line of slope 0.03 in./mA in Figure 20.

Another check is a comparison of the computed pressure gain values for each stage with the measured gain. For the first stage,

$$(GK_y)_1 \times (dP_o/dy)_1 = (5.18 \times 10^{-4}) \times (3.320 \times 10^3) = 1.72$$

This is considerably less than the slope of 2.8 shown on the gain curve of Figure 24. For the second stage,

$$(GK_y)_2 \ (dP_o/dy)_2 = (1.88 \times 10^{-4}) \times (1.48 \times 10^4) = 2.78$$

This compares reasonably with the slope shown for the curves of Figure 19.

The dynamic response of the servovalve without derivative feedback is illustrated in Figure 26. The measured response was 3 dB down at 0.45 Hz as compared with the predicted value of 3 dB down at 0.09 Hz (Figure 11). One explanation for the higher measured response frequency is that the actual effective load spring (K) was higher than the assumed value of K = 5 lb/in. In the test configuration, the bandwidth was affected by several factors that were not accounted for in the model. These include the spool spring, friction in the actuator and derivative piston, and compliance of the fluid displaced by the derivative piston. If a value of K = 25 lb/in. is assumed, much closer agreement is obtained as shown by the solid curves in Figure 26. The test data in Figure 26 indicate a first-order type of response up to 1 or 2 Hz with the phase angle going to -90 degrees and the initial slope of the gain curve approximating -20 dB per decade. Above 2 Hz, however, the phase angle and rate of dropoff in gain give the appearance of [illegible] ponse characteristics.

The performance of the servovalve with derivative feedback was encouraging. As shown in Figure 27, several test points were obtained. At 1 and 5 Hz the gain values fluctuated by 5 and 15 dB, as shown by the pairs of vertical lines. At 0.6 [illegible] Hz, relatively steady gain was observed. The behavior of the actuator in this condition was unstable with the

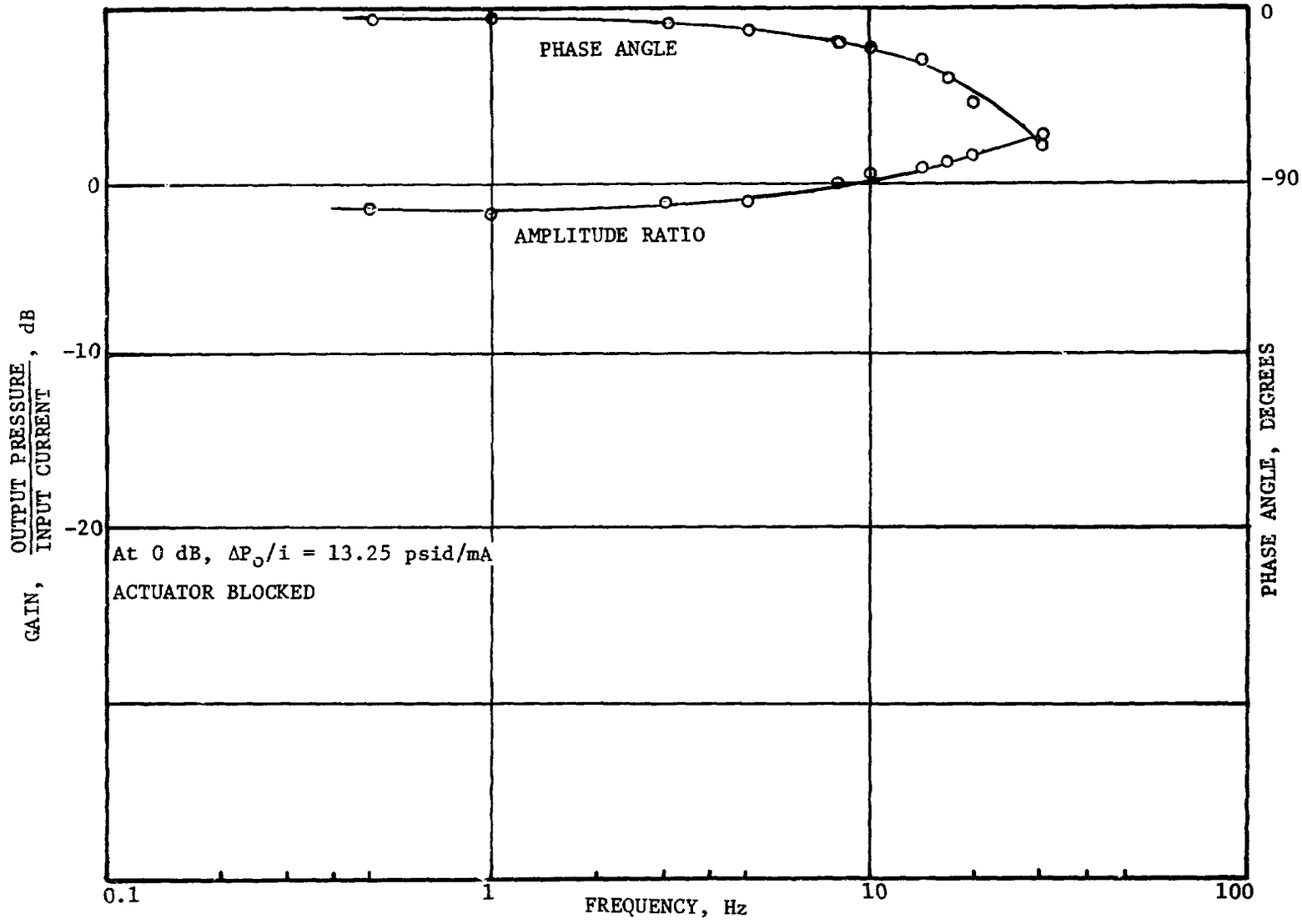

FIGURE 25. AMPLIFIER GAIN BLOCK FLUIDIC RESPONSE

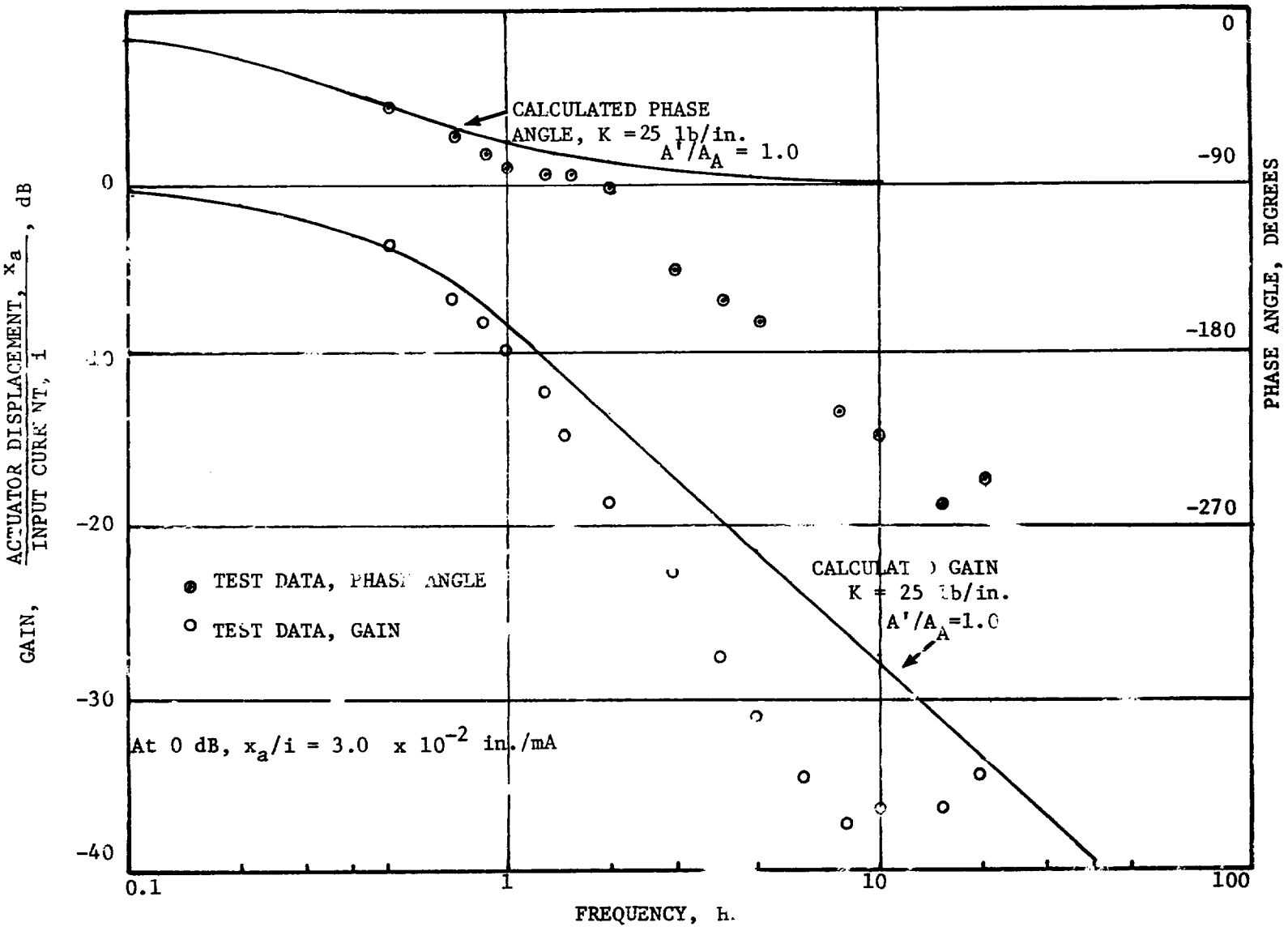

FIGURE 26. ACTUATOR RESPONSE WITHOUT DERIVATIVE FEEDBACK

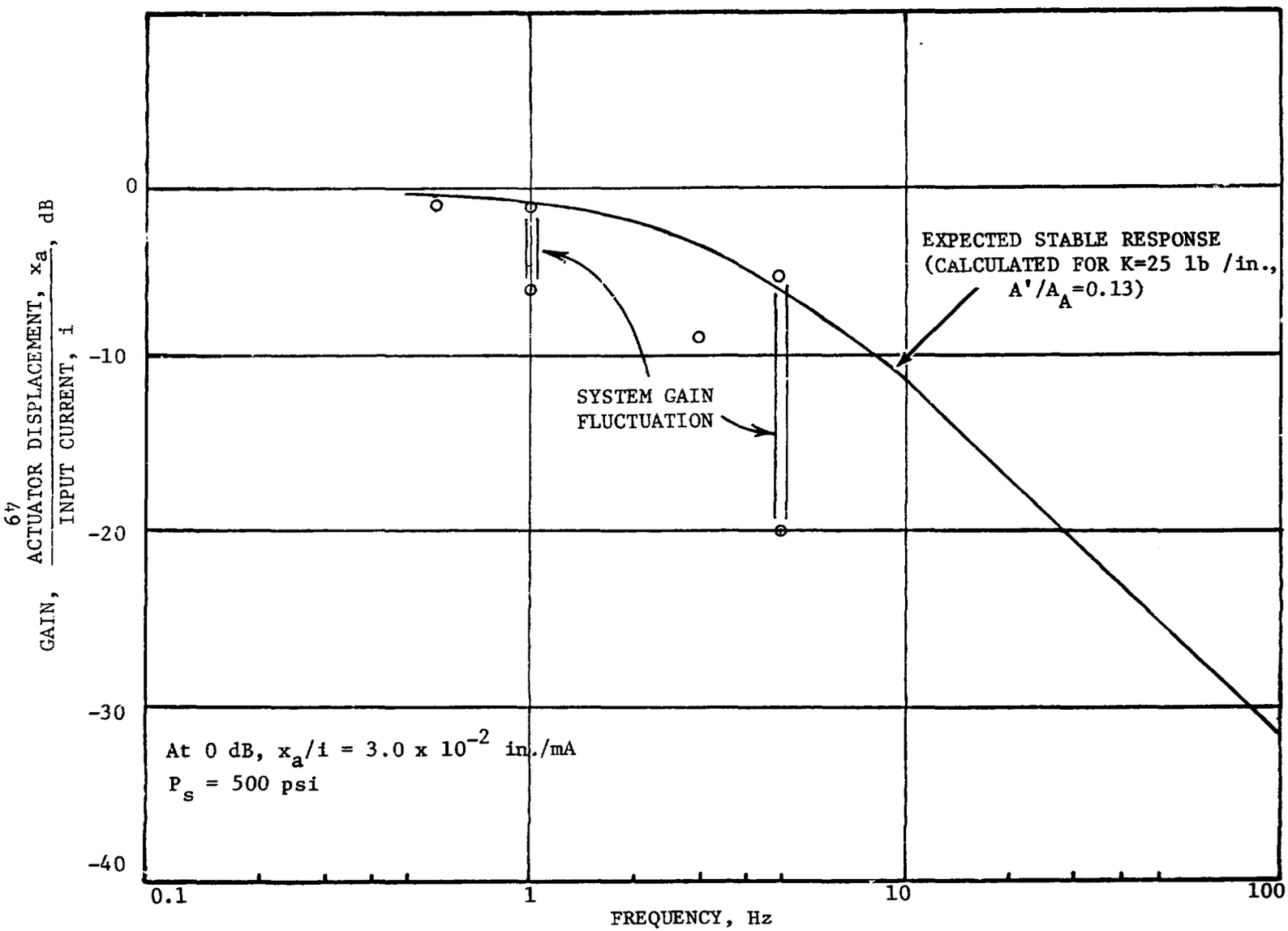

FIGURE 27. ACTUATOR RESPONSE WITH DERIVATIVE FEEDBACK

actuator piston exhibiting a low frequency drift and the phase angle too erratic to be recorded.

The solid line in Figure 27 represents the calculated system response for K = 25 lb/in. and A'/A_A = 0.13. This calculated response is 3 dB down at 3 Hz (which was the design goal for derivative feedback performance) and shows fairly good correlation with the measured performance.

Even though system bandwidth was improved by use of the derivative feedback, instabilities occured that are not accounted for by the calculations performed thus far. In order to obtain better insight into the observed behavior of the servovalve, the system lag and second-order break frequencies were calculated for the assumed K = 25 lb/in. over a range of derivative feedback values (A'/A_A) and plotted in Figure 28. As stated previously, these calculations predict lag frequencies of 0.45 Hz with no derivative feedback (A'/A_A = 1) and 3 Hz with derivative feedback of A'/A_A = 0.13. However, this plot also shows a crossover between the lag and second-order frequencies in the region of A'/A_A = 0.02. The calculations for this region also show erratic behavior of the transfer-function characteristic-equation roots, indicating a zone of possible instability.

The performance parameters of the components that make up the derivative feedback mechanism were evaluated in a static condition. These parameter values (e.g., Q_b/x_b, R_b, k_b) may not remain constant during dynamic system response conditions. If this is the case, then the term K_B is not constant and will vary as a function of input signal frequency. If K_B varies sufficiently, then A'/A_A could change enough to cause the system to operate in the crossover region.

Assuming that the occurrence of this crossover effect is the basis for the observed system instability, it is desirable to design the system so that the crossover region is eliminated or at least does not occur near the computed value of A'/A_A. With this in mind, the system response was calculated for various values of R_ℓ.

If the leakage resistance across the actuator piston (R_ℓ) is decreased, the crossover region does not occur in the range A'/A_A equals

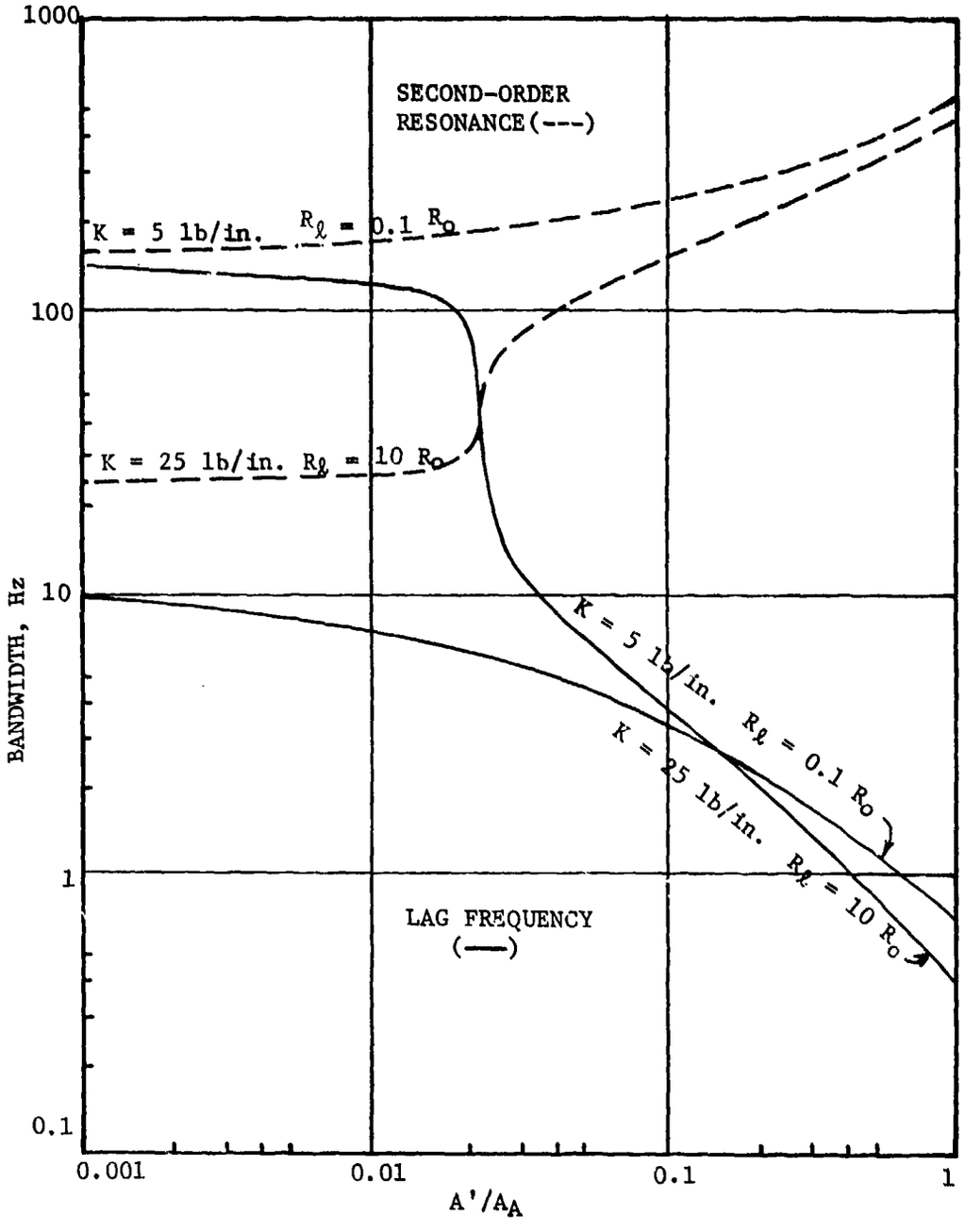

FIGURE 28. EFFECTS OF K AND R_ℓ ON SYSTEM RESPONSE

0.001 to 1. This resistance decrease can be accomplished by a shunt resistor or by allowing more clearance around the actuator piston. This latter approach would have the added benefit of decreasing actuator piston friction.

The effect of decreasing R_ℓ on system response is shown in Figure 28 where system bandwidth versus A'/A_A is plotted for $R_\ell = 0.1\ R_o$ and K = 5 lb/in. These curves show a lag frequency of 0.8 Hz at $A'/A_A = 1$ and 3 Hz at $A'/A_A = 0.13$ without the crossover effect.

CONCLUSIONS

The validity of the mathematical modeling of the servovalve block diagram has been reasonably well established. The servovalve functioned as predicted without derivative feedback, in the areas of accepting dual inputs (hydraulic and electric), position feedback, and frequency response. Use of the positive derivative feedback mechanism resulted in increased bandwidth with unstable operation. Therefore, the performance results obtained were qualitative rather than quantitative. Excessive spool valve friction and dead zone (Figure 8), and actuator friction are among the factors that need improvement. Further study of the elements of the derivative feedback portion of the servovalve should lead to redesign of the system such that the increased bandwidth provided by the derivative feedback can be implemented in a well-behaved device.

RECOMMENDATIONS

A number of problem areas must be addressed before satisfactory stable operation of the servovalve can be attained. The major problem areas and most promising courses of action are:

Splitter Mechanism - Reduce friction and hysteresis by improved seals (such as Teflon-coated O-rings) or eliminate seals by immersing torque motor.

Actuator - Reduce friction while permitting controlled leakage across piston. If necessary, supplement controlled leakage by use of a shunt resistor across actuator ports. Evaluate effects of this redesign on overall system gain.

Derivative Feedback Mechanism - Evaluate and reduce spool friction and dead zone effects. Evaluate spring-like effects of spool flow. Redesign derivative piston area for better match to actuator piston. Evaluate compliance effects in the derivative piston cavity and redesign as required. Reevaluate overall derivative feedback mechanism math model.

It is recommended that the servovalve be reworked as dictated by resolution of the foregoing problem areas. Component tests should be conducted to assure compliance with the performance requirements determined for the appropriate block diagram elements. System level tests should then be carried out to demonstrate the expected improvements in stability and frequency response.

LIST OF SYMBOLS

A_A	actuator piston area, $in.^2$
A_{b1}	derivative piston area, $in.^2$
A_{b2}	spool area, $in.^2$
A'	$A_A - K_B$, $in.^2$
B	load viscous damping, lb sec/in.
C_a	actuator compliance, $in.^3$/psi
G	amplifier gain
i	current, amperes
K_y	jet displacement per pressure difference, in/psi
k_b	spool spring rate, lb/in.
K_B	derivative feedback coefficient, $in.^2$
K	load spring rate, lb/in.
M	load mass, lb sec^2/in.
P_+	amplifier supply pressure, psi
P_s	spool supply pressure, psi
P_b	derivative piston pressure, psi
P_o	amplifier output pressure, psi
P_c	amplifier input pressure, psi
Q_b	spool flow rate, $in.^3$/sec
Q_o	amplifier output flow, $in.^3$/sec
R_o	amplifier output resistance, lb sec/$in.^5$
R_ℓ	actuator leakage resistance, lb sec/$in.^5$

LIST OF SYMBOLS (Cont'd)

R_b	derivative resistance to ground, lb sec/in.^{5}
R'	$R_\ell/(R_\ell + R_o)$
r_x	actuator position feedback ratio = y_{s2}/x_a
s	Laplace operator, sec^{-1}
x_a	actuator displacement, in.
x_b	spool displacement, in.
x_j	jet pipe deflection, in.
x_s	spool position, in.
y_{s1}	first-stage splitter displacement, in.
y_{s2}	second-stage splitter displacement, in.
y/i	torque motor displacement coefficient, in./ampere
Z_ℓ	load impedance, lb/in.
τ	time constant, sec
ζ	damping ratio